

Coordinates Determination of a Single Sensor Node with Respect to a Single Beacon Node using Received Signal Strength (RSS)

Submitted by:
Khalid Bin Salahuddin
ID: 2012-2-60-028
Md. Shafayat Khan
ID: 2012-2-60-044
Amit Kumar Saha
ID: 2012-2-60-057

Supervised by:
Dr. Anisur Rahman
Assistant Professor
Department of Computer Science and Engineering
East West University

**A project submitted in partial fulfillment of the requirements for the
degree of Bachelor of Science in Computer Science and Engineering to the
Department of Computer Science and Engineering
At the**



East West University
Aftabnagar, Dhaka, Bangladesh

Abstract

In this humble project, we studied a certain localization problem in a terrestrial wireless sensor network (WSN). In this regard, we studied the issue of finding a single sensor node (i.e. mobile station, cell phone) under a single beacon node (i.e. BTS). Generally, the localization of a single sensor node in a terrestrial sensor network can be solved using multilateration technique with respect to three or more known beacon nodes. However, there is an area of concern, when the localization of a single sensor node (i.e. mobile station, cell phone) is to be measured with respect to only one known beacon node (i.e. BTS). We aim to solve such a challenge with the help of Received Signal Strength (RSS) Survey. In this project, we have simulated a terrain and created a model based on Received Signal Strength (RSS) Survey that defined the contours of RF coverage in a particular test facility under a single beacon node (BTS). Such a model could possibly give a solution for finding a single sensor node with respect to a single beacon node.

Declaration

We hereby declare that this project was done under CSE497 and has not been submitted elsewhere for requirement of any degree or diploma or for any purpose except for publication.

Khalid Bin Salahuddin

ID: 2012-2-60-028

Department of Computer Science and Engineering
East West University

Md. Shafayat Khan

ID: 2012-2-60-044

Department of Computer Science and Engineering
East West University

Amit Kumar Saha

ID: 2012-2-60-057

Department of Computer Science and Engineering
East West University

Letter of Acceptance

We hereby declare that this thesis is from the aforementioned student's own work and best effort of mine, and all other sources of information used have been acknowledged. This thesis has been submitted with our approval.

Supervisor

Dr. Anisur Rahman

Assistant Professor

Department of Computer Science and Engineering

East West University

Chairperson (Acting)

Dr. Ahmed Wasif Reza

Associate Professor

Department of Computer Science and Engineering

East West University

Acknowledgement

Firstly our most heartfelt gratitude goes to our beloved parents for their endless support, continuous inspiration, great contribution and perfect guidance from the beginning to end.

We owe our thankfulness to our supervisor Dr. Anisur Rahaman for his skilled, almost direction, encouragement and care to prepare myself.

Our sincere gratefulness for the faculty of Computer Science and Engineering whose friendly attitude and enthusiastic support that has given me for four years.

We are very grateful for the motivation and stimulation from my good friends and seniors.

We also thank the researchers for their works that helped us to learn and implement our method to determine the location of a single sensor node with respect to a single beacon node using Received Signal Strength (RSS) Survey.

Abbreviation and Acronyms

BS	Base Station
BSS	Base Station Substation
BTS	Base Transceiver Station
GPS	Global Positioning System
GSM	Global System for Mobile Communication
MS	Mobile Station
MSS	Mobile Switching Station
NLOS	No Line of Sight
RBS	Radio Base Station
RF	Radio Frequency
RF-REM	Radio Frequency – Radio Environment Mapping
RSS	Received Signal Strength
STM	Self-Tuning Method
WLAN	Wireless Local Area Network
WLL	Wireless Local Loop
WSN	Wireless Sensor Network

Table of contents

Abstract.....	I
Declaration.....	II
Letter of Acceptance.....	III
Acknowledgement.....	IV
Abbreviations and Acronyms.....	V
List of Figures.....	IX
List of Tables.....	X

Chapter 1

Introduction

1.1 About Localization.....	1
1.2 About WSN.....	2
1.3 Base Transceiver Station.....	3-4
1.4 RF Site Survey.....	5-6
1.5 Objective of Research.....	6
1.6 Methodology of Research.....	6
1.7 Significance of Research.....	7

Chapter 2

Related Work	8
2.1 RSS Profiling Measurements.....	9
2.2 RSS-Profiling Based Localization.....	10
2.3 Localization Using Signal Strength.....	11
2.4 RF-REM.....	11-12
2.5 Coordinates Determination of Submerged Sensors.....	12-13

Chapter 3

Problem Statement and Solvability

3.1 Problem Domain.....	14-16
3.2 Environmental Constraints.....	16
3.3 Steps involving the RSS Profiling Survey.....	17
3.4 Proposed Test Terrain.....	18-20
3.5 RSS HeatMap Construction from Test Terrain.....	21-24
3.6 Coordinates Computation.....	25

Chapter 4

Experimental Results and Analysis	26-34
--	-------

Chapter 5

Conclusion and Future Work..... 35

References.....36-40

Appendix

Code.....41-56

List of Figures

- Figure: 1.1 Structure of a GSM Network
- Figure: 3.1 Single BTS with four Cell Sectors
- Figure: 3.2 Model Terrain (Increment: 0.25×10^2m)
- Figure: 3.3 Model Terrain (Top View, Increment: 0.25×10^2m)
- Figure: 3.4 Model Terrain (Increment: 1×10^2m)
- Figure: 3.5 Model Terrain (Top View, Increment: 1×10^2m)
- Figure: 3.6 Main Lobe
- Figure: 4.1 RSS HeatMap
- Figure: 4.2 RSS HeatMap (sensor position 1)
- Figure: 4.3 RSS HeatMap (sensor position 2)
- Figure: 4.4 RSS HeatMap (sensor position 3)
- Figure: 4.5 RSS HeatMap (all 3 sensor positions)
- Figure: 4.6 Arc graph (position 1)
- Figure: 4.7 Arc graph (position 1 and 2)
- Figure: 4.8 Arc graph (position 1, 2 and 3)
- Figure: 4.9 Range graph (position 1, 2 and 3)
- Figure: 4.10 Track back graph (position 3)
- Figure: 4.11 Track back graph (position 2)
- Figure: 4.12 Track back graph
- Figure: 4.13 RSS HeatMap (3 localized sensor positions after further calculations)
- Figure: 4.14 RSS HeatMap (final 3 localized sensor positions)

List of Tables

Table: 4.1 RSS data from different sensor positions

Chapter 1:

Introduction

Driven by the growing population of mobile devices and bandwidth-hungry applications, mobile network traffic is set to explode in our near future. Industry research predicts that aggregate wireless traffic will increase by 1000x within the next decade [1]. Positioning in wireless networks is today mainly used for yellow page services. Yet, its importance will grow when emergency call services become mandatory as well as with the advent of more advanced location-based services. It is also plausible that future resource management algorithms may rely on position estimation and prediction [2].

We talked briefly about the Wireless Sensor Network (WSN) technology and about its significance in wireless communications and advances and how localization can be of use in this particular field. Moreover, we presented a general concept for Base Transceiver Station (BTS) and its use in a GSM network.

1.1 About localization

Localization has widely been explored in terrestrial wireless sensor network and various mechanisms have been proposed. Generally these methods can be classified into two categories: range-based and range-free schemes. The former apply inter mode distances to multilateration or triangulation whereas the latter rely on profiling.

Being applicable for almost every scenario, mobile localization based on cellular network has gained increasing interest in recent years. Since received signal strength (RSS) information is available in all mobile phones, RSS-based techniques have become the preferred method for GSM localization. Although the GSM standard allows for a mobile phone to receive RSS information from up to seven base stations (BSs), most of the mobile phones only use the information of the associated cell (BS) as its estimated position. Therefore, the accuracy of GSM localization is seriously limited [3].

1.2 About WSN

Wireless sensor networks (WSNs) are a significant technology attracting considerable research interest. Recent advances in wireless communications and electronics have enabled the development of low-cost, low-power and multi-functional sensors that are small in size and communicate in short distances. Cheap, smart sensors, networked through wireless links and deployed in large numbers, provide unprecedented opportunities for monitoring and controlling homes, cities, and the environment. In addition, networked sensors have a broad spectrum of applications in the defense areas, generating new capabilities for reconnaissance and surveillance as well as other tactical applications [4].

As mobile devices spring up and with the corresponding improvements of wireless communication, localization in mobile networks has become one of the hottest topics in wireless and mobile computing research [5, 6]. However, it is a key problem to acquire sufficient localization accuracy for location-based services (LBSs).

Although the Global Positioning System (GPS) [8] is considered to be the most well-known localization technique, it is not available in many cell phones, requires direct line of sight to the satellites, and consumes a lot of energy. However, WiFi chips, similar to GPS, are not available in many cell phones, and not all cities in the world contain sufficient WiFi coverage to obtain ubiquitous localization.

1.3 Base Transceiver Station (BTS)

A BTS in general has the following parts:

- Transceiver (TRX): Its function is transmission and reception of signals.
- Power Amplifier (PA): It amplifies the receiving signal.
- Combiner: It combines receiving signals so that they could be sent out through a single antenna for a reduction in the number of antenna used.
- Duplexer: It separates sending and receiving signals from/to antenna. It helps to send and receive signals through the same antenna ports.
- Antenna: Used to transmit signals to another entity.
- Alarm Extension System: It collects working status alarms of various units in the BTS and extends them to operations and maintenance monitoring stations.
- Control Function: It Controls and manages various units of BTS, including any software. It helps in On-the-Spot configuration, status changes, software upgrades, etc. are done through the control function.
- Baseband receiver unit (BBxx): Frequency hopping, signal DSP, etc.

A mobile network consists of Mobile Station (MS), BSS, Network Switching Subsystem, Operator Support Subsystem and MSC. All this makes up the GSM mobile network. A BTS, also referred to as the RBS, node B (in 3G Networks) or simply the Base Station or eNB in LTE standard is a system that has the radio transceivers which define a cell and provides wireless communication between users and like mobile phones, computers or WLL phones and a network service provider.

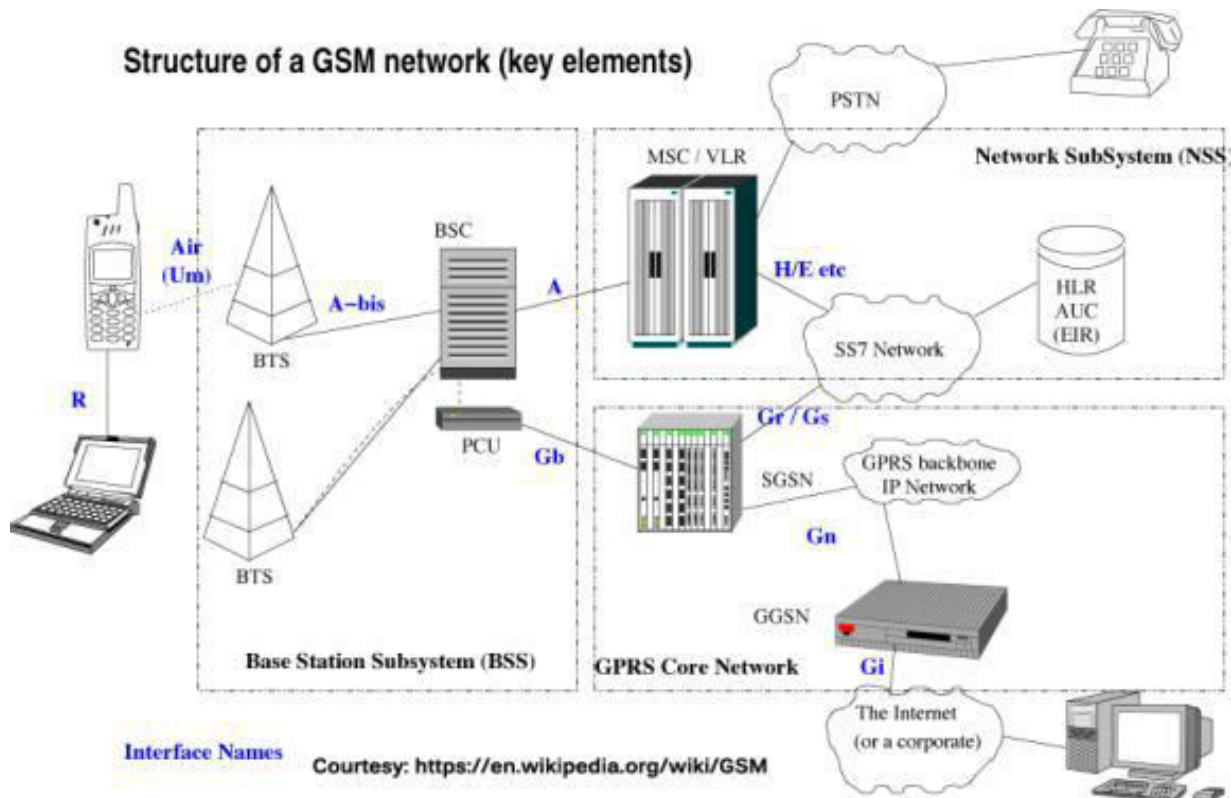


Figure: 1.1 Structure of a GSM Network

A BTS is controlled by a BSC and usually placed in the center of a cell whose transmitting power defines the size of a cell. It has mainly four main parts – power element, a power source (engine/ alternator), a BTS machine, towers and antenna. Each BTS has between 1 to 16 transceivers, depending on the density of users in the cell where each BTS serves a single cell.

The mobile switching station, abbreviated as MSC Server or MSS, is a 2G core network element which controls the network switching subsystem elements. Alternatively or adaptively, MSS can be used in GSM networks as well, if the manufacturer has implemented support for GSM networks in the MSS.

1.4 RF site survey

A wireless site survey (RF survey) is the process of planning and designing a wireless network, to provide a wireless solution that will deliver the required wireless coverage, data rates network capacity, roaming capability and quality of service (QOS) [9]. The survey usually involves a site visit to test for RF interference, and to identify optimum installation locations for access points (BTSs). Wireless site survey can also mean the walk-testing, auditing, analysis or diagnosis of an existing wireless network [9].

Wireless surveys site are typically conducted using computer software that collects analysis RF spectrum characteristics. Before a survey, a site map is imported into a site survey application and calibrated to set scale. During the survey, surveyor walks the facility with a portable computer that continuously records the data. The surveyor uses a GPS receiver that automatically marks the current position when the survey is conducted outside. After the survey is performed, data analysis is performed and survey results are documented in site survey reports generated by the application.

There are three main types of wireless site surveys [10]:

- **Passive Survey:** A site survey application passively listens to WLAN traffic to detect access points, measure signal strength and noise level.
- **Active Survey:** The wireless adapter is associated with one or several access point to measure round-trip time, throughput rates, packet loss and retransmissions.
- **Predictive Survey:** A model of the RF environment is created using tools. It is essential that the correct information on the environment is entered in the RF modeling tool, including location and RF characteristics of barriers like walls or large objects.

In a wireless network, many issues can arise which can prevent the RF signal from reaching all parts of the facility. Examples of RF issues include multipath distortion, hidden node problems and near or far issues. A site survey helps define the contours of RF coverage in a particular facility. It helps to discover regions where multipath distortion can occur, areas where RF interference is high and find solutions to eliminate such issues. A proper site survey provides detailed information that addresses coverage, interference sources, equipment placement, power considerations and wiring requirements. The site survey documentation serves as a guide of network design [11].

1.5 Objective of the research

Our paper discusses the methods of determining the location of a sensor node under a single beacon node along the test surface which would be pre-defined or pre-measured by RSS survey. The traditional networking established various approaches of finding one or more sensor node under multiple beacon nodes [7] but not using only one beacon node; hence we submit here a probable solution to the aforementioned issue.

1.6 Methodology of the research

Here, we developed a certain method which would require some form of networking established between the sensor and beacon node. Then we would take measurements for the RSS of the BTS by the respective sensor node (i.e. cell phone) and calculate its probable distance from the BTS as well as the grid position. Through the combination of these two values, we would find the location of the targeted sensor node. The proposed method is explained in details in chapter 3 and the related calculations are shown in chapter 4.

1.7 Significance of the research

Recent immense growth in wireless networks and related technologies allows its user to be mobile and still get access to information they need. This roaming freedom with the seamless mobility between neighboring base stations facilitates its users to communicate anywhere at any time. While the user is mobile, it is very important for service providers to know the physical location of its users to provide services according to their location.

Self-localization capability is a highly desirable characteristics of WSN. In environmental monitoring applications such as bushfire, surveillance, water quality monitoring and precision agriculture, the measurement data are meaningless without knowing the location from the data are obtained. Sensors with known location information are called anchors and their locations can be obtained by using a global positioning system (GPS), or by installing anchors at points with known coordinates. In applications requiring a global coordinate system, these anchors will determine the location of the sensor network in the global coordinate system [7].

Chapter 2

Related Works

A broad spectrum of solutions, such as received signal strength (RSS), time of arrival (TOA) [12], time difference of arrival (TDOA) [13], and angle of arrival (AOA) [14], has been proposed to attain mobile localization by measuring the radio signal traveling between a mobile terminal and base stations (BSs) [15, 16]. Some researchers have proposed a number of methods including fingerprinting and max-minbox [17]. These techniques, except for RSS, often depend on additional hardware, which means additional cost.

The most well-known localization technique, i.e., the GPS [8], can be categorized as a ToA-based system. Time-based systems require special hardware and therefore are usually deployed on high-end phones. In addition, GPS suffers from two other main problems: 1) availability and 2) power consumption. It requires line of sight to the satellites; therefore, it does not work indoors, and it consumes a lot of power of the energy limited cell phones.

AOA-based systems use triangulation based on the estimated AOA of a signal at two or more base stations to estimate the location of the desired transmitter [18], [19]–[22]. Antenna arrays are usually used to estimate the AOA. Similar to TOA-based systems, AOA-based systems require specialized hardware, which makes them less attractive for a large deployment on cell phones.

City-wide WiFi-based localization has been proposed in [23] and [24], and commercial products are currently available, e.g., [25]. However, WiFi chips, similar to GPS, are not available in the majority of cell phones, and not all cities in the world contain sufficient WiFi coverage to obtain ubiquitous localization.

2.1 RSS profiling measurements

The RSS profiling-based localization techniques [26-30], work by constructing a form of map of the signal strength behavior in the coverage area. The map is obtained either offline by a priori measurements or online using sniffing devices [28] deployed at known locations. They have been mainly used for location estimation in WLANs, but they would appear to be attractive also for wireless sensor networks.

In this technique, in addition to there being anchor nodes (e.g., access points in WLANs) and non-anchor nodes, a large number of sample points (e.g., sniffing devices) are distributed throughout the coverage area of the sensor network.

At each sample point, a vector of signal strengths is obtained, with the j th entry corresponding to the j th anchor's transmitted signal. Of course, many entries of the signal strength vector may be zero or very small, corresponding to anchor nodes at larger distances (relative to the transmission range or sensing radius) from the sample point. The collection of all these vectors provides (by extrapolation in the vicinity of the sample points) a map of the whole region.

The collection of all these vectors provides (by extrapolation in the vicinity of the sample points) a map of the whole region. The collection constitutes the RSS model, and it is unique with respect to the anchor locations and the environment. The model is stored in a central location. By referring to the RSS model, a non-anchor node can estimate its location using the RSS measurements from anchors.

In summary, a number of measurement techniques are available for WSN localization. Which measurement technique to use for location estimation will entirely depend on the specific application of the measurement technique. Typically, localization algorithms based on AOA and propagation time measurements are able to achieve better accuracy than localization algorithms based on RSS measurements. However, that accuracy is achieved at the expense of higher equipment cost.

2.2 RSS-profiling based localization

Given the RSS model constructed using the procedure described in Section 2.1, each non-anchor node unaware of its location uses the signal strength measurements it collects, stemming from the anchor nodes within its sensing region, and thus creates its own RSS finger print, which is then transmitted to the central station. Then the central station matches the presented signal strength vector to the RSS model, using probabilistic techniques or some kind of nearest neighbor-based method, which chooses the location of a sample point whose RSS vector is the closest match to that of the non-anchor node to be the estimated location of the non-anchor node [26]. In this way, an estimate of the location of the non-anchor node can be obtained. The estimate is transmitted to the non-anchor node from the central station. Obviously, a non-anchor node could also obtain the full RSS model from the central station and perform its own location estimation.

The empirical model used in [26] was able to estimate user location with a high degree of accuracy. The median error distance is 2 to 3 meters, about the typical office room. Much of the accuracy can be achieved with an empirical data set of about 40 physical points and about 3 real-time signal strength samples (at each base station). It is important, however, that the empirical data set contain data corresponding to multiple user orientations at each location. The main limitation of the empirical model is that significant effort is needed to construct the Signal Strength data set for each physical environment of interest (each floor, each building etc.). Furthermore, the data collection process may need to be repeated in certain circumstances, e.g., when a base station is relocated.

The accuracy of this technique depends on two distinct factors: the particular technique used to build the RSS model, with the resultant quality of that model, and the technique used to fit the measured signal strength vector from a non-anchor node into the appropriate part of the model. In comparison with distance-estimation based techniques, the RSS-profiling based techniques produce relatively small location estimation errors [26].

2.3 Localization using signal strength

In [31], Elnahrawy et al. proposed several area-based localization algorithms using RSS profiling; these algorithms are area based because instead of estimating the exact location of the non-anchor node, they simply estimate a possible area that should contain it. Two different performance parameters apply: accuracy, or the likelihood that an object is within the area, and precision, i.e., the size of the area. Ref. [31] also considered three different techniques for the area based algorithms, viz., single point matching, area based probability and Bayesian networks. The performance of all three algorithms was compared with the point based algorithm of [26]. The conclusion was that all algorithms performed similarly, with a fundamental limit existing in the case of the RSS-profiling based localization algorithms, a conclusion also consistent with that of [32].

2.4 RF-REM

The performance of RF-REM construction methods clearly varies with the number of measurements and with measurement distribution across scenarios, which can occur in practice with respect to directional transmitter. It has been shown that clustering of measurements in the main lobe of the transmitter antenna notably decreases the performance of all construction methods, especially of the direct methods if the application goal is finding the white spaces in the entire geographical area. Moreover, although direct RF-REM construction is more often considered than the indirect construction, it has been shown that a more accurate RF-REM can be constructed already from small number of randomly distributed measurements by using an indirect construction method with a semi-empirical propagation model taking into account the characteristics of the transmitter and the operating environment.

Modelling of the transmitter antenna proved to be of particularly great importance, although it introduces increased computational complexity, but this can be in practice efficiently addressed by using parallel processing techniques [33].

The proposed STM [33] takes into account the characteristics of the operating environment and performs estimation of the transmitter parameters, i.e. its location, antenna diagram, antenna azimuth, transmit power, as well the parameters of the propagation model to obtain the best match between the available measurements and the predicted signal levels.

The main contribution of [33] is a new indirect RF-REM construction method that is well-suited also to collection of measurements points using a participatory sensing approach. Its characteristics can be summarized as follows: (i) the method takes into account the characteristics of the Tx, i.e. transmit power, antenna diagram, its azimuth and tilt, (ii) the signal measurements are applied for the propagation model calibration, and (iii) the method relies on the semi-empirical propagation model in which the empirical propagation model is complemented with the available information about the radio propagation environment including the digital elevation model and clutter information of the geographical area of interest.

2.5 Coordinates determination of submerged sensors

A method of determining the underwater distances between beacon and sensor nodes has been presented [34] using combined radio and acoustic signals, which has better immunity from multipath fading. Moreover, Cayley-Menger determinant is used to determine the coordinates of the nodes where none of nodes have a priori knowledge about its location.

To determine the coordinates of the submerged sensors, the proposed method [34] assumes at least three sensors and a floating beacon. It is also assumed that the distance measurement between the beacon and sensors are possible. In the marine environment, a boat or a buoy can be used as a beacon and sensors could be deployed in the water. While measuring the multiple distances between the beacon and sensors, those locations of the beacon are assumed to be in a plane, which is approximately parallel to the plane created by the three sensors.

The objective of localization algorithms is to obtain the exact position or coordinates of all the sensor nodes by measuring distances between beacon and them. Only measurements available here to compute is the distance and typically it is considered as optimization problem where objective functions to be minimized have residuals of the distance equations. The variables of any localization problem are the 3D coordinates of the nodes. In principle more number of distance equations are needed than number of variables to solve this kind of problem. However, this approach known as degree of freedom analysis may not guarantee the unique solution in a nonlinear system.

The method is relatively simple but precise enough when both the beacon and sensors are capable of transmitting/receiving radio and acoustic signals. To be precise, the beacon should be capable of acoustic (transmit (T_x) & receive (R_x)) and radio (transmit: (T_x)) only. On the other hand, sensors should be capable of acoustic (transmit (T_x) & receive (R_x)) and radio (receive (R_x)) only.

The assumption that with the use of appropriate sensors, the depth h can be measured [35]. Time taken for the acoustic signal to travel from beacon to sensors is t_{ij} . Sensor nodes send back the time $t_{ij}(\text{travel})$ with individual sensor's ID to the beacon using acoustic signal. Beacon node computes the distance between the beacon and the appropriate sensors as $d_{ij} = v_A \times t_{ij}(\text{travel})$. Here, v_A is average acoustic signal speed.

After that, with the help of the Cayley-Menger determinant technique, the positions of the respective sensor nodes are calculated.

The proposed method [34] is for a specific configuration and scenario, where a single moving beacon node is necessary to determine the coordinates of the sensor nodes.

Chapter 3

Problem Statement and Solvability

In this following chapter, we'll be discussing in detail the methods leading to the localization of a single sensor node (i.e. mobile station) with the help of a solitary Base Transceiver Station (BTS) using Received Signal Strength (RSS) Survey.

The chapter begins with a detailed outlay of the problem domain and the environmental constraints surrounding the problem. Later, a terrain was simulated and the basis for creating a RSS HeatMap for the stimulated terrain using Friis transmission equation and free-space path loss equation were explained in full details.

3.1 Problem domain

A solitary traditional BTS can only find the possible quadrant of a sensor node when they establish a link with that BTS. Our problem scenario arises for an area under the coverage of a solitary BTS where the sensor node (i.e. mobile station) wants to know its probable two-dimensional location within the BTS's coverage area. Usually, in city and urban area there are multiple BTSs which can perform localization using one of AOA, triangulation or multilateration method.

Our case resumes with a worse case situation with the possibility of or combination of such reasons as in geographical, political, economic or technological drawbacks where a certain area happens to have a solitary BTS with a certain credible range. There is a question of interest as to how a solitary BTS is going to perform localization in such a scenario. The answer to this question is that a solitary BTS can only find out the quadrant position in which the sensor node resides. But this paper shows that the location of a particular sensor node can be made more precise inside a particular quadrant with our proposed method.

A base transceiver station can have 1 to 16 cell sectors. Generally, it possess up to three to four cell sectors operating under four different directional antenna. Each cell sectors covers an area with a wedge shaped area with each having the same angular span for the same BTS.

In figure 3.1, we have divided our test BTS coverage area into four cell sectors (quadrants) where each quadrant spans exactly by 90 degrees.

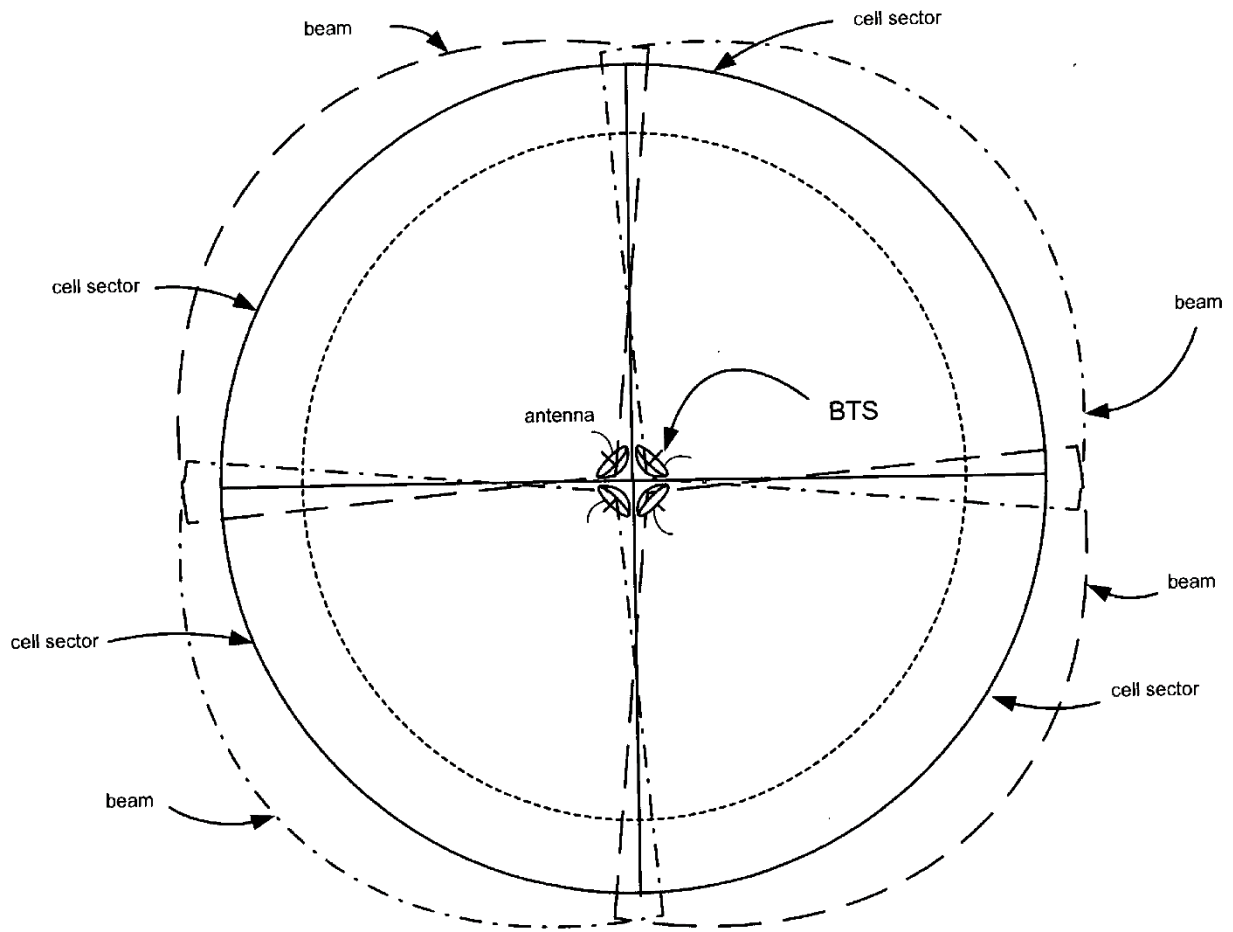


Figure: 3.1 Single BTS with four Cell Sectors

To find a narrowed down location of a sensor in our problem scenario established where apart from a single BTS and a single cell phone the coverage area has a distinctive terrain, we are only going to consider the coordinate values of the area along the XY surface for simplicity. Moreover the RSS Survey data were also collected beforehand to find the respective RSS value of squared grid on the two-dimensional XY coverage surface.

3.2 Environmental constraints

For our proposed method, the size of the area we have worked with is a 2x2 km area and is represented with a digital elevation model with the resolution of 100 m. Even for such a small area, this should produce a total of 400 grids (given that there are no grids where surveillance cannot be performed because of natural or artificial hindrance). These grids should be manually explored at certain positions within each grid and their corresponding RSS received by the exploring mobile unit should be acknowledged and recorded as per each grid. Thus, it can be assumed that the calculated signal level at each 100x100 m RF-REM point is very close to real situation. However, for a hilly terrain, a terrain with forestry or a lake inside it, it would quite difficult to arrive at every grid positions per 100 m for RSS checking due to lack of flat or solid ground.

With the RSS and output power of base station (BS), it is possible to estimate the distance between the mobile device and BS using Friis transmission equation. The problem is that the distance d_{ij} is calculated with the RSS. In the propagation, signal sometimes suffer interference and shadow fading, and distance d_{ij} would not always be the exact distance between base station (BS) and the mobile station (MS) and so cannot be considered always for this method. However, for areas with distorted RSS, different technique need to be taken into consideration to determine the distance d_{ij} .

The main idea is to make good use of the cell information, to locate a two-dimensional position and minimize the influence of disturbance, barriers, or NLOS errors, for example, on performance.

3.3 Steps involving the RSS profiling survey

Firstly a predictive approach should be followed. A model of the RF environment is created using tools. It is essential that the correct information on the environment is entered in the RF modeling tool, including location and RF characteristics of barriers like walls or large objects.

To make sure that the correct information on the environment were entered in the RF modeling tool, a passive approach should be followed soon after, where a site survey application should be deployed in the problem field which passively listens to WLAN traffic to detect access points, measure signal strength and noise level.

A step-by-step approach for performing the aforementioned tasks are detailed below:

- Obtain a facility diagram in order to identify the potential radio frequency obstacles within the RF environment.
- Visually inspects the facility to look for potential barriers (hills or mountains) or the propagation radio frequency signals and identify metal rocks and places like lakes or rivers.
- Identify user areas that are highly used and the once that are not used.
- Determine preliminary access points (AP) locations.
- Perform the actual surveying in order to verify the AP location. Make sure to use the same AP model for the survey that is used in production. While the survey is performed, relocate APs as needed and re-test.
- Document the findings. Record all the individual locations (two-dimensional) and log of all the signal readings (RSSs).
- Build a two-dimensional Heatmap based upon the findings.

3.4 Proposed test terrain

We have used Matlab R2016a for coding and implementing the simulation of a 20x20 meshgrid terrain. We have built Environmental Peaks and Pits on our model surface over certain grids and tried to create an impression for hilly, forestry and lake like elemental presence that could be present under any BTS. Although, we were not able to draw a BTS within the proposed terrain, but the surface's $(X, Y, Z) = (0, 0, 0)$ coordinate should be imagined as the point where the BTS actually is. A remainder to the readers here is this is not the whole terrain that is under the coverage of a solitary BTS. However, this terrain merely represents only a certain area of one of the four quadrants that was divided by the 4 directional antenna used in cell sectoring each with a 90° span.

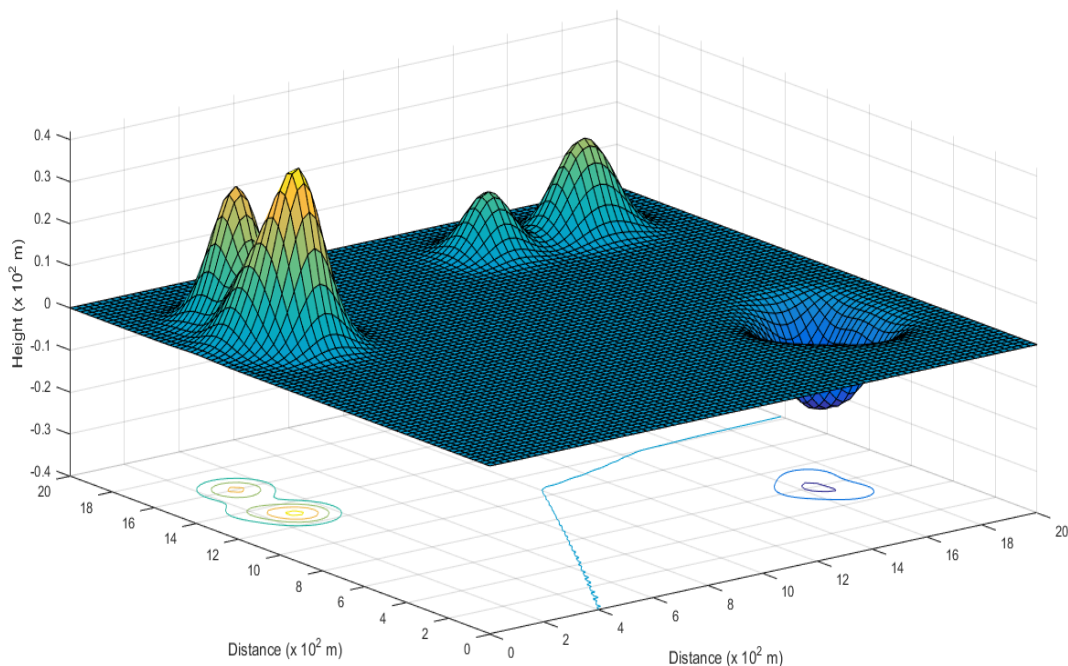


Figure: 3.2 Model Terrain (Increment: $0.25 \times 10^2 m$)

In figure 3.2, the meshgrid defined has an increment of $0.25 (x 10^2 m)$ from $0 (x 10^2 m)$ to $20 (x 10^2 m)$. A total of six peaks and three pits were simulated over the terrain using the surf function. A function named peak provided the necessary logic for building the peaks and the pits at specific locations within the meshgrid. The coloring of the grids were done based on the height with yellow portions having the highest possible heights and the blue portion representing the lowest ones in terms of height.

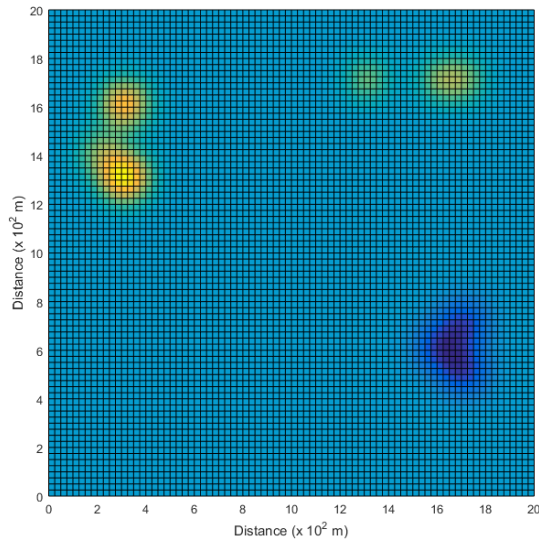


Figure: 3.3 Model Terrain (Top View, Increment: $0.25 \times 10^2 m$)

Figure 3.3, gives a top view of the meshgrid, that have been explained in details a while ago, with an increment of $0.25 (x 10^2 m)$ from $0 (x 10^2 m)$ to $20 (x 10^2 m)$. However, if we considered this as the basis for RSS Survey, there is a massive total of 6400 grids within the simulated terrain.

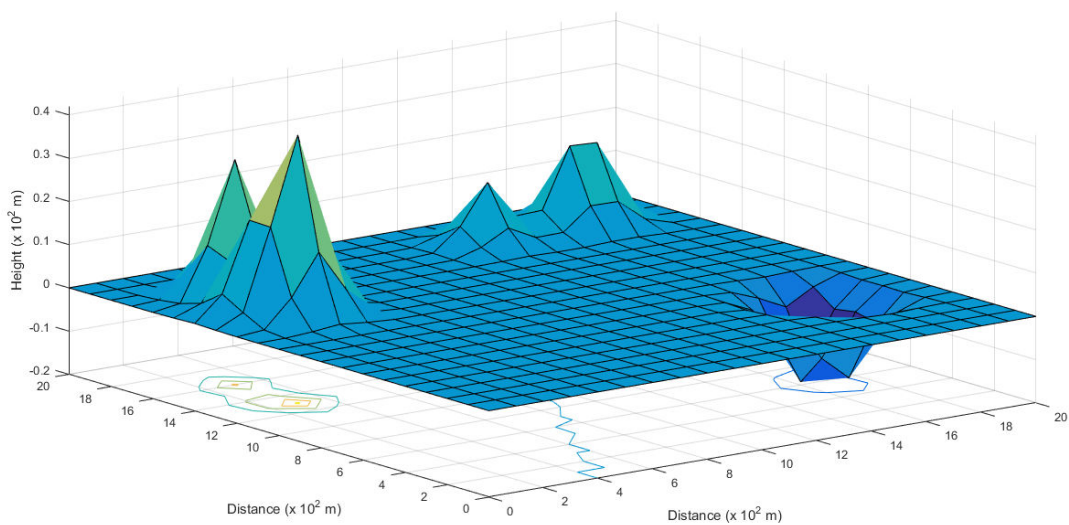


Figure: 3.4 Model Terrain (Increment: $1 \times 10^2 m$)

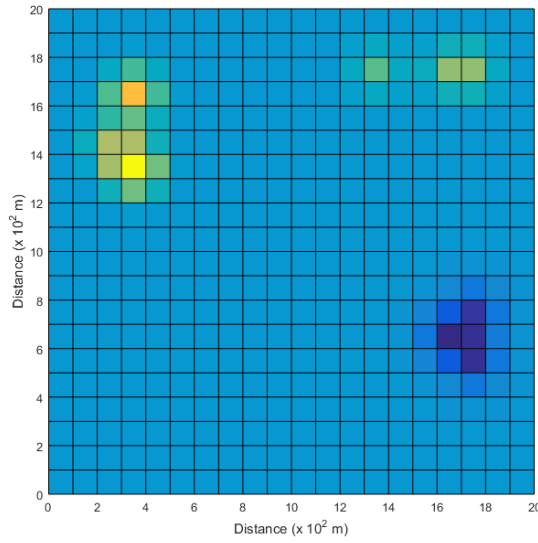


Figure: 3.5 Model Terrain (Top View, Increment: $1 \times 10^2 m$)

In figure 3.4, the meshgrid defined has an increment of $1 (x 10^2 m)$ from $0 (x 10^2 m)$ to $20 (x 10^2 m)$. Hence, less number of grids were produced. 400 grids to be précised. Later in figure 3.5, a top view image of this meshgrid with an increment of $1 (x 10^2 m)$ from $0 (x 10^2 m)$ to $20 (x 10^2 m)$ was plotted.

Figure 3.2 and 3.3 were created for better visualization and understanding of the test Terrain. On the other hand, figure 3.4 and 3.5 are created in accordance with the RSS Heatmap, with an increment of $1 (x 10^2 m)$. All these will be discussed in more details later on in this Chapter, as well as in chapter (4) of this paper.

3.5 RSS HeatMap construction from test terrain

Approach for RSS HeatMap construction. The area of interest is divided into grids, and the HeatMap is constructed using the RSS fingerprint locations inside the grid cell. No extra overhead is required for RSS HeatMap construction. The grid cell length parameter can be used to trade off accuracy and scalability, as well as computational complexity. Larger cells lead to lower accuracy, but they reduce the computational complexity due to the reduced number of cells and vice-versa.

After we made the test terrain in a 20x20 grid, we individually then defined the 400 grids with the assigned RSS survey values using both Friis transmission equation and free-space path loss equation since raw data were not available. We recorded these 400 values and assigned them into a Matrix using Matlab coding. After successful simulation, Matlab provided us with a HeatMap of the test Terrain based on the RSS reading for individual grids as shown in figure 3.3.

Friis transmission equation (3.1):

$$P_r = P_t - FSPL_{d,f}$$

$$P_r = P_t - (20 \log_{10} d + 20 \log_{10} f + 92.45)$$

P_r = Recieved Signal Strength (RSS) by the Mobile Station

P_t = Transmitted Signal Strength (TSS) from the Base Transceiver Station

d = distance between Base Transceiver Station and Mobile Station

f = signal frequency of the Base Transceiver Station

Free-space path loss equation (3.2):

$$FSPL = \left(\frac{4\pi d}{\lambda}\right)^2 = \left(\frac{4\pi df}{c}\right)^2$$

d = distance between Base Transceiver Station and Mobile Station

f = signal frequency of the Base Transceiver Station

c = speed of light in vacuum, 3×10^8 m/s

λ = wavelength of the transmitted signal of the Base Transceiver Station

Free-space path loss equation (3.3):

$$FSPL (dB) = 10 \log_{10} \left(\left(\frac{4\pi df}{c} \right)^2 \right)$$

$$FSPL (dB) = 20 \log_{10} \left(\frac{4\pi df}{c} \right)$$

$$FSPL (dB) = 20 \log_{10} d + 20 \log_{10} f + 20 \log_{10} \left(\frac{4\pi}{c} \right)$$

$$FSPL (dB) = 20 \log_{10} d + 20 \log_{10} f - 147.55$$

d = distance in meters (m)

f = signal frequency in Hertz (Hz)

Free-space path loss equation (3.4):

$$FSPL (dB) = 20 \log_{10} d + 20 \log_{10} f + 92.45$$

d = distance in meters (Km)

f = signal frequency in Hertz (GHz)

We will be using a combination of Friis transmission equation (3.1) along with Free-space path loss equation (3.4) for the buildup to our RSS HeatMap.

Variables used for the test Terrain:

$f = 900 \text{ MegaHertz (MHz)}$

$d = 100 \text{ meter (m) per increment}$

$P_t = 39 \text{ decibel (dB)}$

Logics behind the terrain heat map on the basis of RSS survey are mainly to maintain the logical spread of values along the surface using Friis transmission equation (1) along with the help of Free-space path loss (4). Here, the diagonal grids go furthest in terms of maintaining the better signal strengths than surrounding grids signal strengths because of the presence of a main lobe in the radiation pattern.

Main lobe:

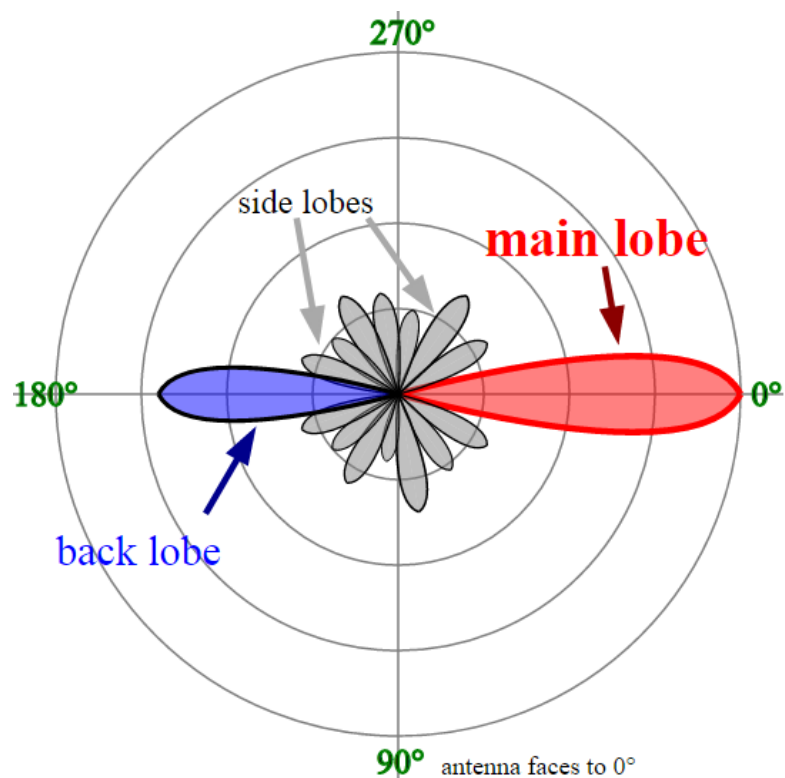


Figure: 3.6 Main Lobe

In a radio antenna's radiation pattern, the main lobe, or main beam is the lobe containing the maximum power. This is the lobe that exhibits the greatest field strength. The radiation pattern of most antennas show the above "lobes" at different angles, direction where the radiated signal strength reaches a maximum, separated by "nulls", angles at which the radiation falls to zero. In the directional antenna in which the objective is to emit the radio waves in one direction, the lobe in that direction is designed to have higher field strength than the others on a graph.

The surrounding grids in front of the hilly (top left distorted field in the simulated terrain) areas, feet of mountainous areas covering grids sometimes have better signal strengths than usual because of multipath propagation when signals from opposite directions collide with each other with the same phase value and vice-versa. Moreover, the grids those are behind the mountains are being deprived of their usual signal mark because of NLOS. Hence we would see a big drop in the RSS values over those grids.

Same rationalization was being implemented around and over the forestry areas (top right distorted field in the simulated terrain).

Around the pits (impression of a Lake – bottom right distorted field in the simulated terrain) the presence of water on the grids means signal propagation will not be smooth and that signals will be more or less absorbed by water which is why the grids are given very low signal strength values as well as the surrounding grids which are also constantly getting affected from the wayward reflection and multipath propagation of the signal because of the lake.

Considering all of these factors mentioned above we have finally created our HeatMap based on RSS for a 20x20 meshgrid space with a total of 400 grids. An image of the RSS HeatMap was provided in chapter (4).

3.6 Coordinates computation

Our proposed method works in two simple steps:

- An offline RSS HeatMap construction phase and
- An online tracking phase.

During the offline phase, a probabilistic RSS HeatMap is constructed, where the RSS from the solitary cell tower at given locations in the area of interest is estimated. The purpose of this offline phase is to construct the RSS HeatMap for the solitary cell tower (BTS) at each location in the fingerprint area. Typically, this requires the surveyor to stand at each location in the fingerprint for a certain period of time to collect enough samples to construct the RSS HeatMap. However, this will increase the fingerprint construction overhead significantly.

During the online tracking phase, the RSS HeatMap is used to calculate the most probable fingerprint location at which the user may be standing at that instance. If the online tracking phase discovers a single grid as a probable fingerprint location of the user, it tells the user a two-dimensional positional information about his or her whereabouts with respect to the discovery of a single probable grid. Otherwise, the person is advised to start moving in a straight line in any specific direction, for a finite amount of time, for another probable fingerprint location data. This approach strives to determine the possible cluster within the RSS HeatMap where the user might be by eliminating areas of no interest.

Chapter 4

Experimental Results and Analysis

A simulation of the proposed method to determine the location of a single sensor node (MS) with respect to a fixed single beacon node (BTS) using RSS HeatMap. The experiment was designed based on two-dimensional space. The Beacon node was placed at X, Y (0, 0) surface of the simulated terrain and the Sensor node was moved through three positions starting from (9.5, 2.5) to (11.5, 5.5) and later to (13.5, 7.5). This proposed method has been simulated using Matlab R2016a.

Sensor position	RSS	Actual grid location
1	-52.64 dB	(10, 3)
2	-54.64 dB	(12, 6)
3	-55.67 dB	(14, 8)

Table: 4.1 RSS data from different sensor positions

To simulate the proposed method we have taken into consideration the following scenario as mentioned above. However, a single dataset can contain a minimum of one to finite different positions for the sensor node (i.e. mobile station) which when needed should be moved in a straight line to aid for the localization calculation. To calculate the coordinates of the actual sensor positions in terms of the grid they are placed at, we need the inter distances between the different positions of the sensor node and their corresponding positions from the beacon node.

The inter distances between the different sensor positions as it moved along a straight line can be calculated from the average walking speed of a human, also taking into consideration, the time it took for the sensor node (i.e. mobile station) to move from one position to the next position. For this particular problem, we have taken a value of 2.82 unit as the inter-position distance between the three sensor positions.

As per research, the preferred walking speed at which a human choose or tend to walk is about 1.4 m/s (5.0 Km/h; 3.1 mph) [36-38]. We have considered the form of 1.4 m/s as the preferred walking speed for the user availing our localization technique.

In figure 4.1, the RSS HeatMap we have created for our simulated terrain has been shown.

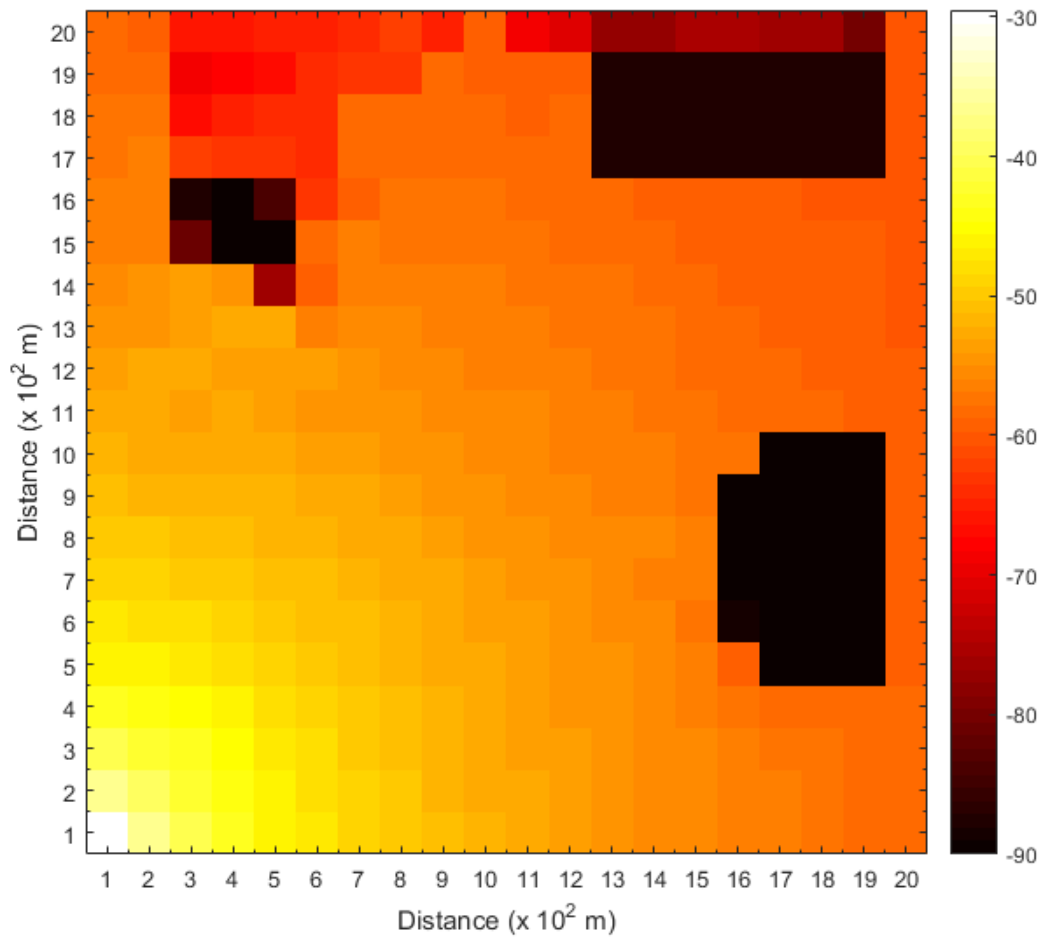


Figure: 4.1 RSS HeatMap

Initially, a RSS HeatMap was plotted based for the sensor node (position 1) considering the returned RSS data sent from the sensor node (i.e. mobile station) to the beacon node (i.e. BTS). Similarly, respective RSS HeatMap were plotted based on the RSS data sent from the sensor node (position 2 and position 3). All these have been shown graphically from figure 4.2-4.5 as well as with the combined RSS HeatMap for all the three sensor positions.

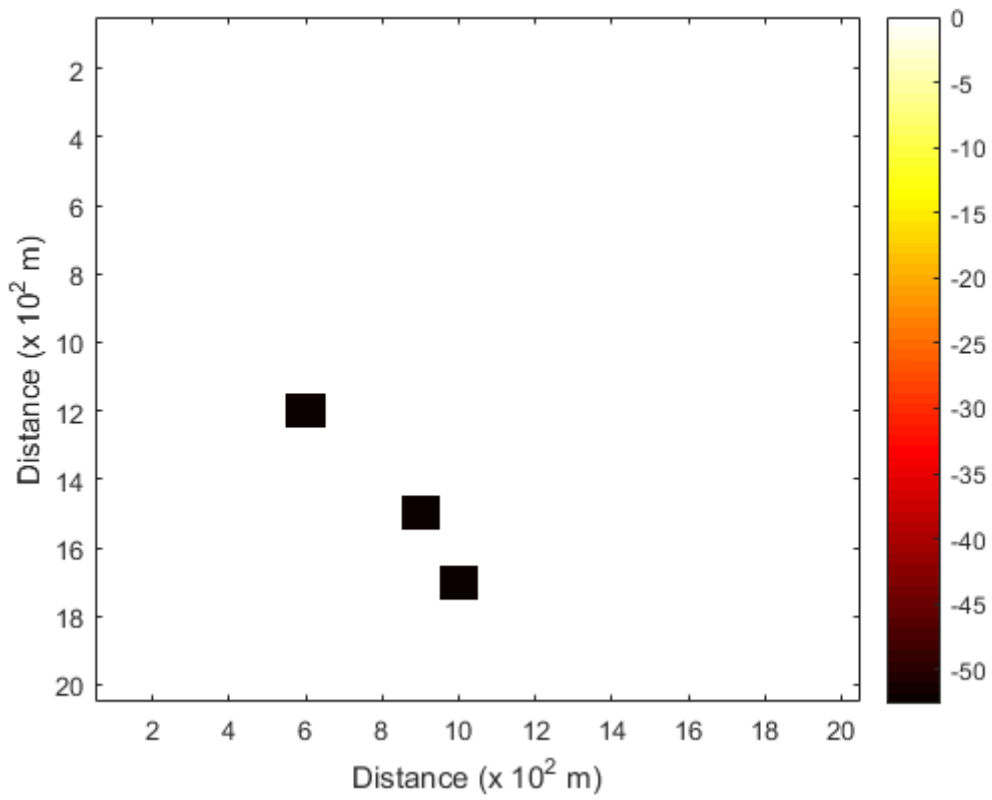


Figure: 4.2 RSS HeatMap (sensor position 1)

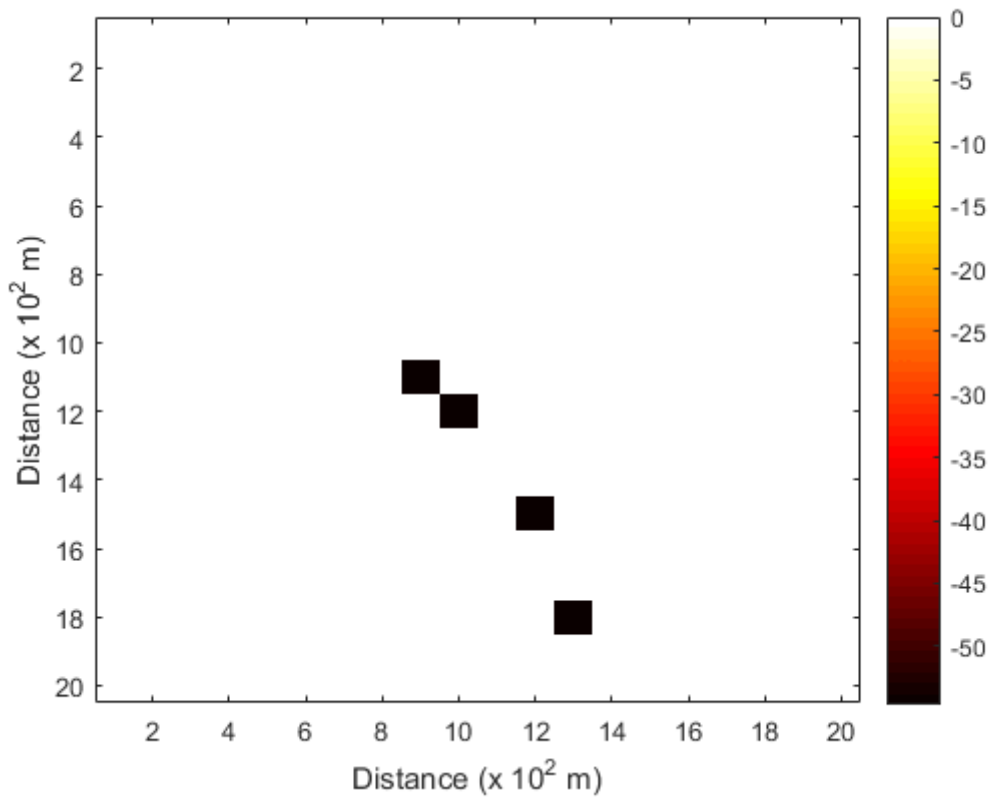


Figure: 4.3 RSS HeatMap (sensor position 2)

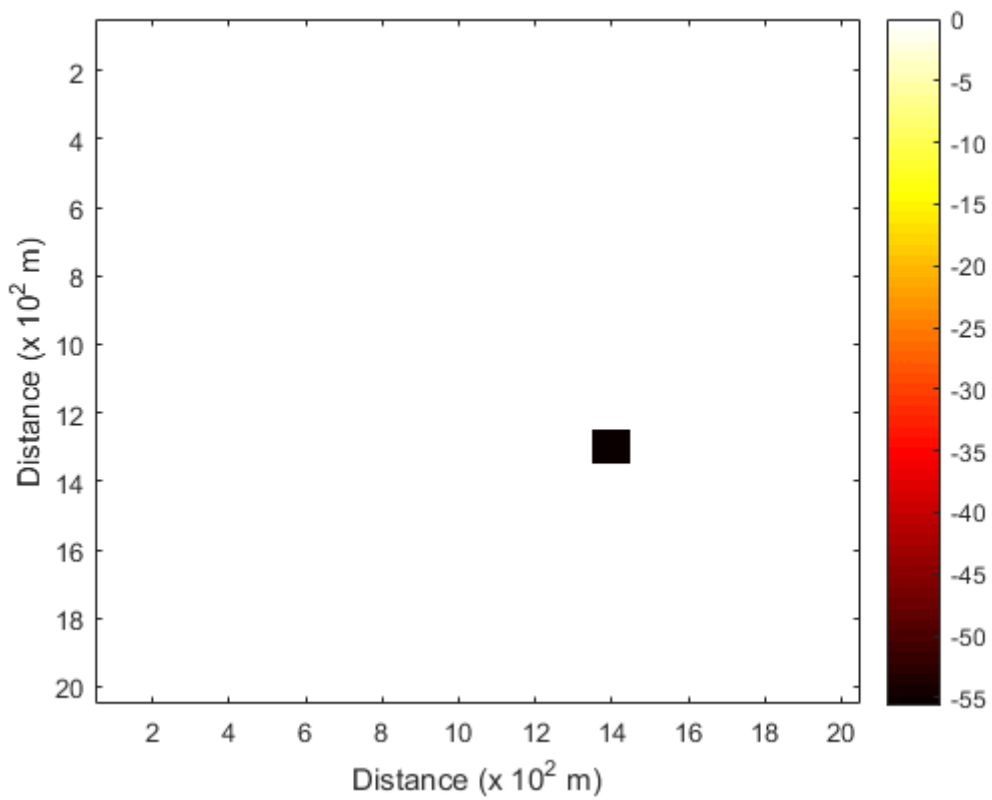


Figure: 4.4 RSS HeatMap (sensor position 3)

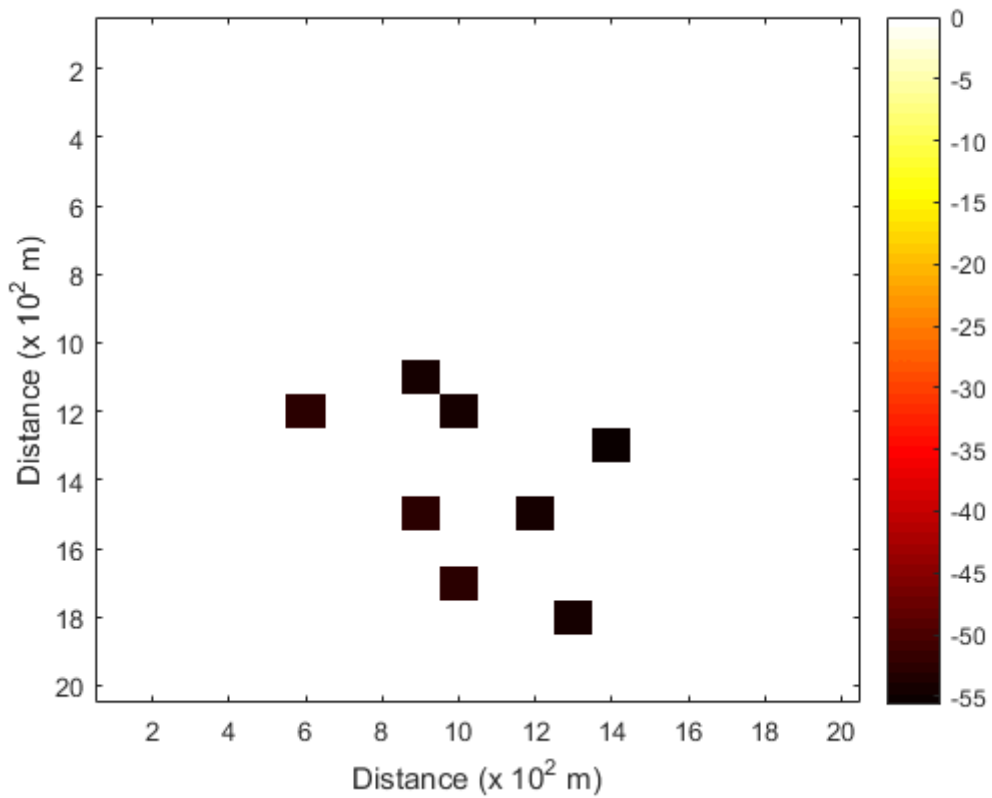


Figure: 4.5 RSS HeatMap (all 3 sensor positions)

Further calculations might provide more evidence for the exact locations of the initial sensor positions before a certain distinctive grid was finally found. Hence, a footprint for the user can be created. The calculations necessary for this has been shown graphically from figure 4.6-4.11.

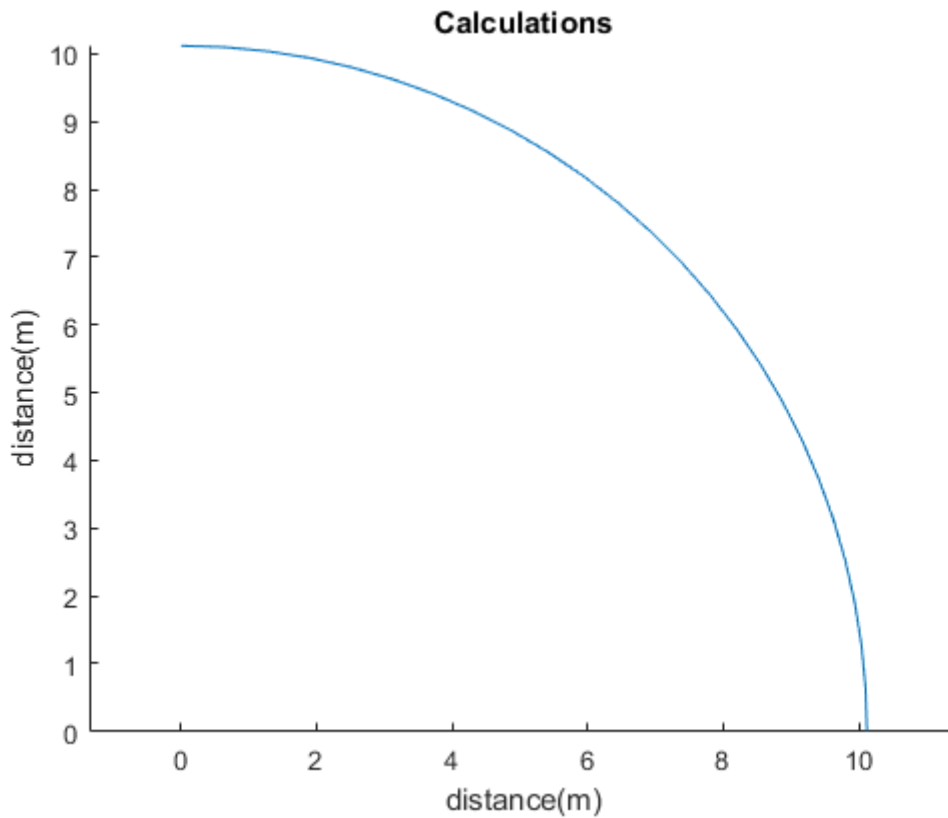


Figure: 4.6 Arc graph (position 1)

Figure 4.6 was drawn using the distance between the beacon node and the first position of the sensor node calculated using Friis transmission equation (4) from the RSS reading returned by the sensor node in that instance.

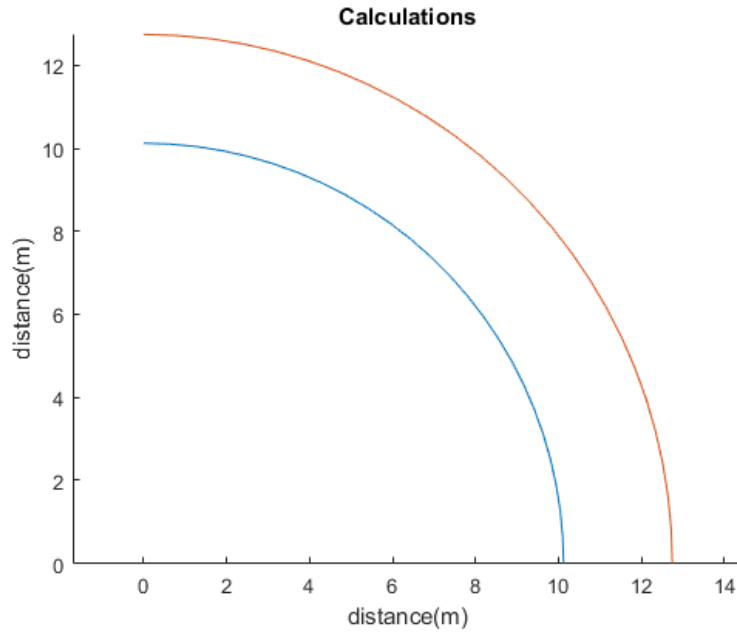


Figure: 4.7 Arc graph (position 1 and 2)

Figure 4.7 was drawn using the distance between the beacon node and the second position of the sensor node calculated using Friis transmission equation (4) from the RSS reading returned by the sensor node in that instance.

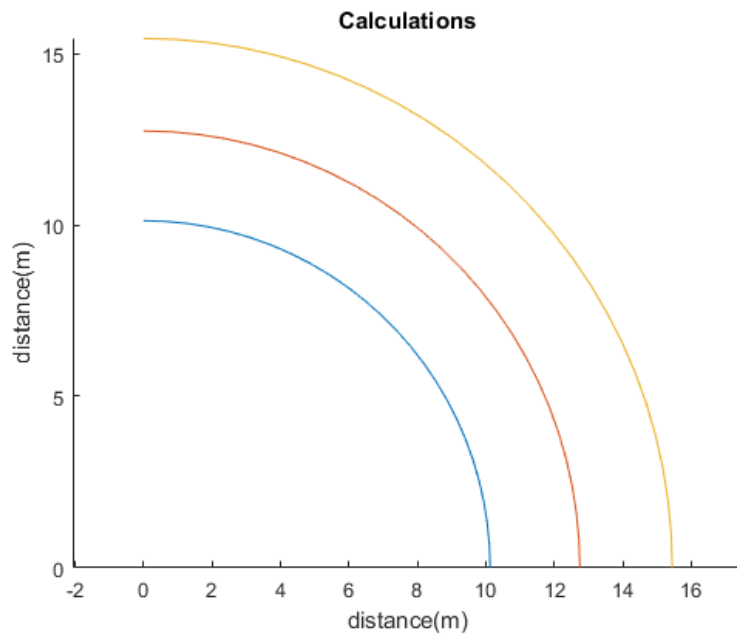


Figure: 4.8 Arc graph (position 1, 2 and 3)

Figure 4.8 was drawn using the distance between the beacon node and the third position of the sensor node calculated using Friis transmission equation (3.1) from the RSS reading returned by the sensor node in that instance.

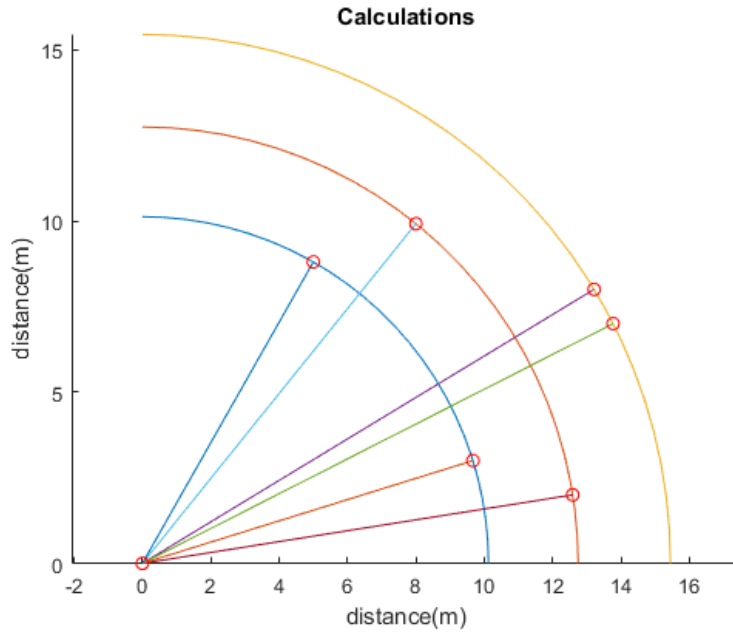


Figure: 4.9 Range graph (position 1, 2 and 3)

Figure 4.9 was drawn using all the distances between the beacon node and all the position of the sensor node accumulated above. This graph further gives all the separate ranges for each arc created using the three distances and considering the initially projected grids in figure 4.5.

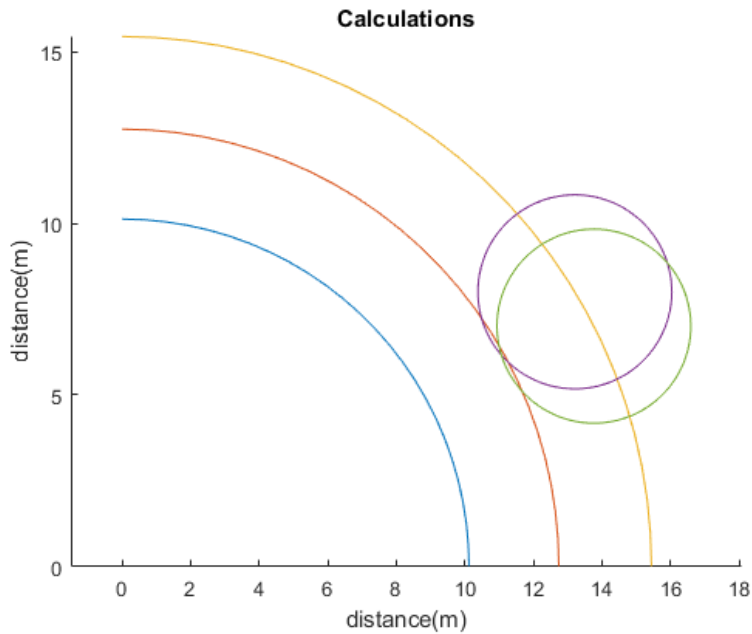


Figure: 4.10 Track back graph (position 3)

In figure 4.10, the track back method was initiated using the distance between the second position and the third position of the sensor node. A circle is drawn using the aforementioned distance from the lower and the upper bounds of the third position of the sensor.

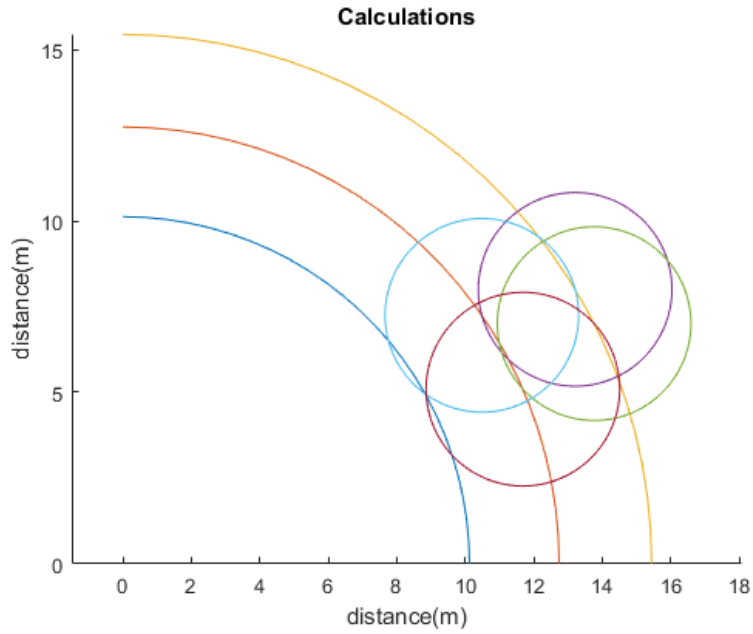


Figure: 4.11 Track back graph (position 2)

In figure 4.11, a circle was drawn using the distance between the first and the second position of the sensor node from the lower and the upper bounds of the second position of the sensor.

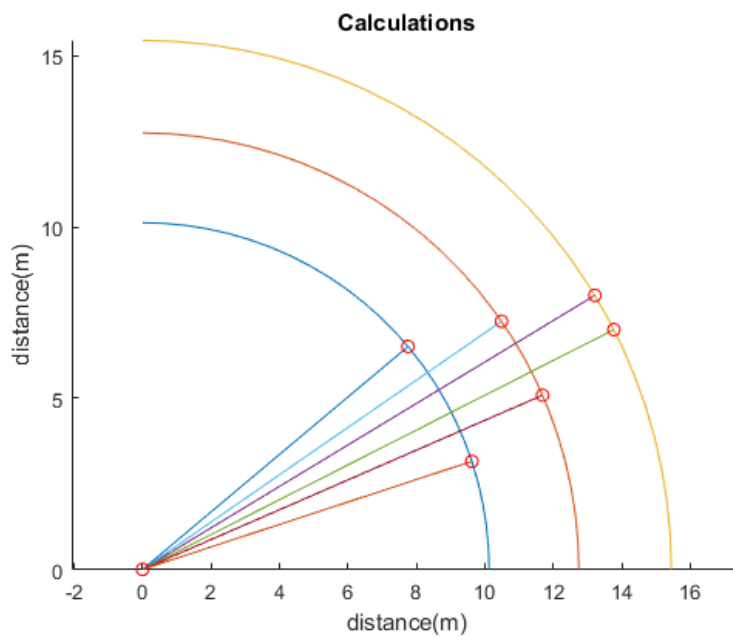


Figure: 4.12 Track back graph

In Figure 4.12, a graph was drawn accumulating the figures 4.9-4.11. This graph further narrow down the ranges for each projected grid positions of the sensor node.

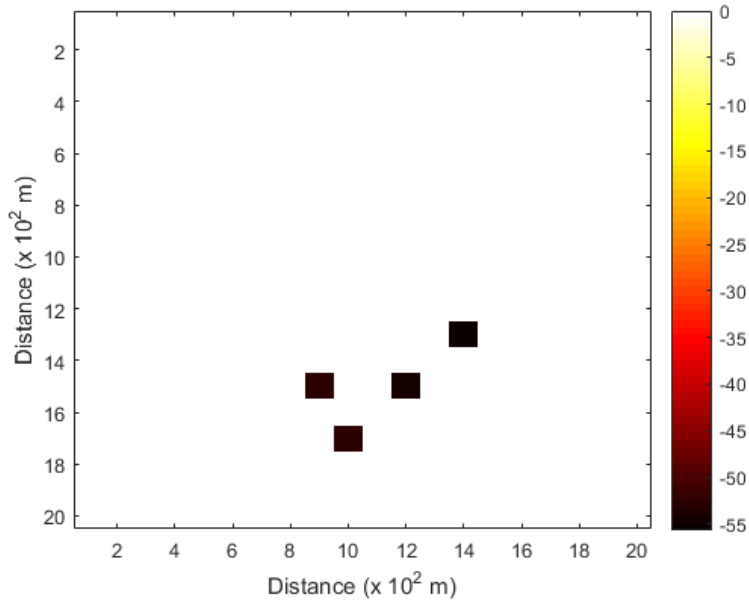


Figure: 4.13 RSS HeatMap (3 localized sensor positions after further calculations)

Figure 4.13 further makes use of both figure 4.12 and figure 4.5. This is a more precise predicted grid localization.

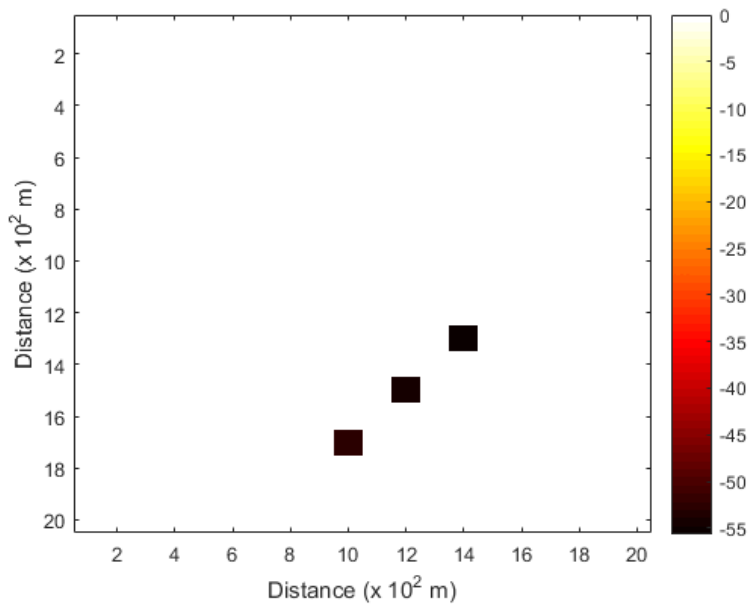


Figure: 4.14 RSS HeatMap (final 3 localized sensor positions)

However, if we consider that the sensor node moved in a straight line for the three positions of the sensor node. One of the predicted grid for the initial position of the sensor node can be eliminated which would result in the true three predicted grids.

Chapter 5

Conclusion and Future Work

We have successfully implemented our method on the simulated terrain to determine the two-dimensional location of a single sensor node with respect to a single beacon node using RSS HeatMap. The data for the created RSS HeatMap were taken on the basis of Friis Transmission Equation (3.1) while considering the Free-Space Path Loss Equation (3.4). However, a proper RSS HeatMap should be made considering both the theoretical model and the real-life recorded data. This would produce a far better RSS HeatMap than the one with which we have worked upon in this paper. For our proposed method, we have considered 100 m^2 area under each grid. However, if the area under each grid is reduced any further, far better accuracy could be achieved but such a policy would be more cumbersome for carrying out any physical RSS survey. There would be increase in computation complexity as well. Moreover, we were short on resources while creating the simulated terrain based only on the Friis transmission equation (3.1) since there are numerous environmental elements. Furthermore, we introduced only one specific terrain and based our model around it but working with more challenging terrains is possible with our proposed method.

This proposed method using RSS HeatMap could be of much better use if the computational complexities that are present in this time are reduced by using Clustering algorithms through Machine Learning in the future.

References

- [1] Qualcomm Inc., The 1000x data challenge, <https://www.qualcomm.com/1000x>, 2014.

- [2] Fredrik Gustafsson and Fredrik Gunnarsson, “Mobile Positioning using wireless Networks: Possibility and fundamental limitation based on available wireless networks measurements”, proceedings of the IEEE vol. 22 issue 4, July 2005, PP 41-53

- [3] Huiyu Liu, Yunzhou Zhang, Xiaolin Su, Xintong Li, and Ning Xu, “Mobile Localization Based on Received Signal Strength and Pearson’s Correlation Coefficient”, Hindawi Publishing Corporation, International Journal of Distributed Sensor Networks, Volume 2015, Article ID 157046, 10 pages

- [4] C. –Y. Chong, S. Kumar, “Sensor Networks: Evolution, Opportunities, and Challenges”, proceedings of the IEEE 91 (8) (2003) 1247-1256

- [5] M. Anisetti, C. A. Ardagna, V. Bellandi, E. Damiani, and S. Reale, “Map-based location and tracking in multipath outdoor mobile networks,” IEEE Transactions on Wireless Communications, vol. 10, no. 3, pp. 814–824, 2011.

- [6] K. Yu, I. Sharp, and Y. J. Guo, Ground-Based Wireless Positioning, John Wiley & Sons, 2009.

- [7] Guoqiang Mao, Baris Fidan, Brian D.O. Anderson, “Wireless Sensor Networks Localization techniques Computer Networks”. 51 (2007), PP 2529-2553.

- [8] P. Enge and P. Misra, "Special issue on GPS: The global positioning system," Proc. IEEE, vol. 87, no. 1, pp. 3–15, Jan. 1999.
- [9] Joshua Bardwell; Devin Akin (2005). "Certified Wireless Network Administrator Official Study Guide (Third edition)". McGraw-Hill, pp. 479–547. ISBN 978-0-07-225538-
- [10] Shawn M. Jackman, Matt Swartz, Marcus Burton and Thomas W. Head (2011). "Certified Wireless Design Professional Official Study Guide.". John Wiley & Sons. , pp. 392–396,403–418. ISBN 978-0-470-76904-1.
- [11] Wireless Site Survey, <https://www.cisco.com>, 686666
- [12] J. Shen, A. F. Molisch, and J. Salmi, "Accurate passive location estimation using TOA measurements," IEEE Transactions on Wireless Communications, vol. 11, no. 6, pp. 2182–2192, 2012.
- [13] J. Saloranta and G. Abreu, "Solving the fast moving vehicle localization problem via TDOA algorithms," in Proceedings of the 8th Workshop on Positioning, Navigation and Communication (WPNC '11), pp. 127–130, IEEE, Dresden, Germany, April 2011.
- [14] M. Dakkak, A. Nakib, B. Daachi, P. Siarry, and J. Lemoine, "Indoor localization method based on RTT and AOA using coordinates clustering," Computer Networks, vol. 55, no. 8, pp. 1794–1803, 2011.
- [15] C. Gentile, N. Alsindi, R. Raulefs et al., "Multipath and NLOS mitigation algorithms in Geolocation Techniques", pp. 59–97, Springer, New York, NY,USA, 2013.

- [16] M. Ibrahim and M. Youssef, "CellSense: an accurate energy efficient GSM positioning system," *IEEE Transactions on Vehicular Technology*, vol. 61, no. 1, pp. 286–296, 2012.
- [17] M. Bshara, U. Orguner, F. Gustafsson, and L. Van Biesen, "Fingerprinting localization in wireless networks based on received signal- strength measurements: a case study on WiMAX networks," *IEEE Transactions on Vehicular Technology*, vol. 59, no. 1, pp. 283–294, 2010.
- [18] S. Tekinay, "Special issue on wireless Geolocation systems and services," *IEEE Commune Mag.*, vol. 36, no. 4, Apr. 1998.
- [19] E. Elnahrawy, J. Austen-Francisco, and R. P. Martin, "Adding angle of arrival modality to basic RSS location management techniques," in *Proc. IEEE ISWPC*, 2007, pp. 464–469.
- [20] E. Elnahrawy, J.-A. Francisco, and R. P. Martin, "Poster abstract: Bayesian localization in wireless networks using angle of arrival," in *Proc. 3rd ACM Conf. Embedded Network SenSys*, 2005, pp. 272–273.
- [21] P. Biswas, H. Aghajan, and Y. Ye, "Integration of angle of arrival information for multimodal sensor network localization using semidefinite programming," in *Proc. 39th Asilomar Conf. Signals, Syst. Comput.*, 2005.
- [22] M. Li and Y. Lu, "Angle-of-arrival estimation for localization and communication in wireless networks," in *Proc. 16th EUSIPCO*, 2008.
- [23] Y.-C. Cheng, Y. Chawathe, A. LaMarca, and J. Krumm, "Accuracy characterization for metropolitan-scale Wi-Fi localization," in *Proc. 3rd Int. Conf. Mobile Syst., Appl. Services MobiSys*, New York, 2005, pp. 233–245.

- [24] I. Smith, J. Tabert, A. Lamarca, Y. Chawathe, S. Consolvo, J. Hightower, J. Scott, T. Sohn, J. Howard, J. Hughes, F. Potter, P. Powledge, G. Borriello, and B. Schilit, "Place lab: Device positioning using radio beacons in the wild," in Proc. 3rd Int. Conf. Pervasive Comput., 2005, pp. 116–133.
- [25] Skyhook Wireless. [Online]. Available: <http://www.skyhookwireless.com>
- [26] P. Bahl, V. Padmanabhan, RADAR: an in-building RF-based user location and tracking system, in IEEE INFOCOM, vol. 2, 2000, pp. 775-784.
- [27] P. Prasithsangaree, P. Krishnamurthy, P. Chrysanthis, On indoor position location with wireless LANs, in The 13th IEEE International Symposium on Personal, Indoor and Mobile Radio Communications, vol. 2, 2002, pp. 720-724.
- [28] P. Krishnan, A. Krishnakumar, W.-H. Ju, C. Mallows, S. Gamt, A system for LEASE: location estimation assisted by stationary emitters for indoor RF wireless networks, in: IEEE INFOCOM, vol. 2, 2004, pp. 1001-1011.
- [19] Teemu Roos , Petri Myllymäki , Henry Tirri, A Statistical Modeling Approach to Location Estimation, IEEE Transactions on Mobile Computing, v.1 n.1, p.59-69, January 2002 [doi>10.1109/TMC.2002.1011059]
- [30] S. Ray, W. Lai, I. Paschalidis, Deployment optimization of sensor-net-based stochastic location-detection systems, in: IEEE INFOCOM 2005, vol. 4, 2005, pp. 2279-2289.
- [31] E. Elnahrawy, X. Li, R. Martin, The limits of localization using signal strength: a comparative study, in: First Annual IEEE Conference on Sensor and Ad-hoc Communications and Networks, 2004, pp. 406-414.
- [32] R. Battiti, M. Brunato, A. Villani, Statistical learning theory for location fingerprinting in wireless LANs, Informatica e Telecomunicazioni, University of Trento, Tech. Rep. DIT 02-086, October 2002.

- [33] Marko Pesko, Tomaz Javornik, Luka Vidmar, Andrej Kosir, Mitja Stular and Mihael Mohor, The indirect self-tuning method for constructing radio environment map using omnidirectional or directional transmitter antenna, *EURASIP Journal on Wireless Communications and Networking* (2015) 2015:50, DOI 10.1186/s13638-015-0297-2
- [34] Anisur Rahman, Vallipuram Muthukkumarasamy, Elankayer Sithirasenan, Coordinates Determination of Submerged Sensors Using Cayley-Menger Determinant, 2013 IEEE International Conference on Distributed Computing in Sensor Systems, vol. 00, no. , pp. 466-471, 2013, doi:10.1109/DCOSS.2013.62
- [35] I. Vasilescu, K. Kotay, D. Rus, M. Dunbabin, and P. Corke, "Data collection, storage, and retrieval with an underwater sensor network," in *Proceedings of the 3rd international conference on Embedded networked sensor systems*, 2005, pp. 154-165.
- [36] Browning, R. C., Baker, E. A., Herron, J. A. and Kram, R. (2006). "Effects of obesity and sex on the energetic cost and preferred speed of walking". *Journal of Applied Physiology*. 100 (2): 390–398. doi:10.1152/jappphysiol.00767.2005
- [37] Betty J. Mohler, William B. Thompson, Sarah H. Creem-Regehr, Herbert L. Pick Jr, William H. Warren Jr, (2007). "Visual flow influences gait transition speed and preferred walking speed". *Experimental Brain Research*. 181 (2): 221–228. doi:10.1007/s00221-007-0917-0. PMID 17372727
- [38] Levine, R. V. & Norenzayan, A. (1999). "The Pace of Life in 31 Countries". *Journal of Cross-Cultural Psychology*. 30 (2): 178–205. doi:10.1177/0022022199030002003

Appendix

Code

(Matlab R2016a)

#Model Terrain Function

```
function z = peak(a,b,c,k,x,y);  
f = 'c*exp(-k*(((x-a)^2)+((y-b)^2)))';  
z = eval(vectorize(f));
```

#Model Terrain (Increment: $0.25 \times 10^2 m$)

```
[x,y]=meshgrid(0:0.25:20);  
  
h1=peak(3,13,0.40,0.9,x,y);  
h2=peak(3,16,0.32,0.9,x,y);  
h3=peak(2,14,0.15,1,x,y);  
L1=peak(17,5,-0.15,0.9,x,y);  
L2=peak(17,7,-0.14,0.9,x,y);  
L3=peak(16,6,-0.145,0.85,x,y);  
f1=peak(17,17,0.14,1,x,y);  
f2=peak(16,17,0.145,1,x,y);  
f3=peak(13,17,0.145,1,x,y);  
  
surf(x,y,h1+h2+h3+L1+L2+L3+f1+f2+f3);  
  
zlabel('Height (x 10^2 m)')  
ylabel('Distance (x 10^2 m)')  
xlabel('Distance (x 10^2 m)')
```

#Model Terrain (Increment: $1 \times 10^2 m$)

```
[x,y]=meshgrid(0:1:20);

h1=peak(3,13,0.40,0.9,x,y);
h2=peak(3,16,0.32,0.9,x,y);
h3=peak(2,14,0.15,1,x,y);
L1=peak(17,5,-0.15,0.9,x,y);
L2=peak(17,7,-0.14,0.9,x,y);
L3=peak(16,6,-0.145,0.85,x,y);
f1=peak(17,17,0.14,1,x,y);
f2=peak(16,17,0.145,1,x,y);
f3=peak(13,17,0.145,1,x,y);

surfc(x,y,h1+h2+h3+L1+L2+L3+f1+f2+f3);

zlabel('Height (x 10^2 m)')
ylabel('Distance (x 10^2 m)')
xlabel('Distance (x 10^2 m)')
```

#RSS HeatMap

```
cdata= [-58.50 -58.86 -65.50 -65.50 -64.77 -64.77 -63.98 -62.59 -64.90 -65.80 -69.00 -71.00 -
77.00 -77.30 -75.23 -75.70 -76.10 -76.60 -80.20 -60.44;

-58.46 -58.40 -68.50 -68.20 -66.67 -64.02 -63.53 -63.30 -58.93 -58.93 -59.13 -59.28 -
70.00 -80.00 -85.00 -90.00 -90.00 -88.00 -88.00 -60.40;

-57.02 -57.00 -67.00 -65.00 -64.00 -63.81 -58.71 -58.11 -58.89 -58.80 -58.93 -58.64 -
70.00 -80.00 -85.00 -78.00 -85.00 -85.00 -88.00 -60.35;

-56.93 -56.81 -62.35 -63.00 -63.50 -63.70 -58.68 -58.30 -58.05 -58.19 -58.50 -58.12 -
70.00 -80.00 -85.00 -78.00 -85.00 -87.00 -87.00 -60.33;
```

-56.59 -56.59 -88.00 -90.00 -84.00 -63.10 -58.87 -57.82 -57.82 -57.59 -58.10 -58.41 -
58.12 -58.93 -59.14 -59.33 -59.72 -59.81 -59.92 -60.31;

-56.17 -56.00 -81.00 -90.00 -90.00 -57.92 -56.60 -57.00 -57.09 -57.75 -57.51 -58.01 -
58.23 -58.50 -58.93 -59.03 -59.33 -59.72 -59.75 -60.29;

-55.25 -54.60 -54.00 -55.00 -76.00 -59.01 -55.89 -56.55 -56.57 -56.83 -57.09 -57.49 -
57.87 -58.20 -58.50 -58.93 -59.13 -59.33 -59.74 -60.15;

-55.00 -54.60 -54.00 -53.00 -53.00 -56.00 -55.88 -55.54 -55.92 -56.46 -56.83 -56.44 -
57.34 -57.87 -58.17 -58.38 -58.93 -59.13 -59.63 -60.12;

-54.07 -53.01 -53.01 -53.01 -53.01 -53.68 -54.76 -55.41 -55.54 -55.94 -56.12 -56.83 -
56.54 -57.59 -58.33 -58.70 -58.71 -59.11 -59.33 -60.09;

-53.31 -53.31 -53.31 -53.31 -53.69 -54.07 -54.42 -54.76 -55.08 -55.41 -55.89 -56.12 -
56.88 -57.01 -57.59 -58.52 -58.61 -58.72 -59.11 -59.72;

-52.48 -52.48 -52.48 -52.48 -52.89 -53.31 -53.69 -54.07 -54.76 -55.08 -55.41 -56.00 -
56.33 -57.03 -57.64 -57.59 -58.66 -58.73 -59.11 -59.72;

-51.56 -51.56 -51.56 -51.56 -52.02 -52.48 -53.31 -53.69 -54.07 -54.76 -55.08 -55.34 -
56.00 -56.57 -57.09 -57.64 -90.00 -90.00 -90.00 -59.33;

-50.55 -50.55 -50.55 -50.55 -51.56 -52.02 -52.48 -52.89 -53.69 -54.07 -54.76 -55.41 -
55.54 -55.77 -56.57 -90.00 -90.00 -90.00 -90.00 -59.33;

-49.38 -49.38 -49.38 -49.97 -50.55 -51.56 -51.56 -52.48 -53.31 -53.69 -54.42 -54.76 -
55.41 -56.00 -56.57 -89.00 -90.00 -90.00 -90.00 -59.33;

-48.04 -48.04 -48.04 -49.38 -49.38 -50.55 -51.56 -51.56 -52.48 -53.31 -54.07 -54.76 -
55.08 -55.54 -57.70 -89.00 -90.00 -90.00 -90.00 -59.00;

```
-46.46 -46.46 -46.46 -48.04 -48.71 -49.38 -50.55 -51.56 -52.02 -52.89 -53.69 -54.42 -  
54.76 -55.41 -56.67 -59.00 -90.00 -90.00 -90.00 -59.00;
```

```
-44.42 -44.52 -44.52 -46.46 -48.04 -49.38 -49.97 -50.55 -51.56 -52.48 -53.31 -54.07 -  
54.76 -55.41 -56.00 -57.00 -58.00 -58.12 -58.66 -58.76;
```

```
-42.03 -42.03 -44.52 -44.52 -46.46 -48.04 -49.38 -50.55 -51.56 -52.48 -53.31 -54.07 -  
54.76 -55.41 -56.00 -56.57 -57.23 -57.59 -58.46 -58.76;
```

```
-38.50 -38.50 -42.03 -44.52 -46.46 -48.04 -49.38 -50.55 -51.56 -52.48 -53.31 -54.07 -  
54.76 -55.41 -56.00 -55.70 -57.19 -57.59 -58.46 -58.76;
```

```
-32.48 -38.50 -42.03 -44.52 -46.46 -48.04 -49.38 -50.55 -51.56 -52.48 -53.31 -54.07 -  
55.00 -55.55 -56.17 -56.80 -57.19 -57.66 -58.46 -58.76];
```

```
colormap('hot')
```

```
imagesc(cdata)
```

```
colorbar
```

```
ylabel('Distance (x 102 m)')
```

```
xlabel('Distance (x 102 m)')
```


#RSS HeatMap (Sensor Position 2)

```
cdata= [0 0 0 0 0 0 0 0 0 0 0 0 0 0 0 0 0 0 0 0 0;
        0 0 0 0 0 0 0 0 0 0 0 0 0 0 0 0 0 0 0 0 0;
        0 0 0 0 0 0 0 0 0 0 0 0 0 0 0 0 0 0 0 0 0;
        0 0 0 0 0 0 0 0 0 0 0 0 0 0 0 0 0 0 0 0 0;
        0 0 0 0 0 0 0 0 0 0 0 0 0 0 0 0 0 0 0 0 0;
        0 0 0 0 0 0 0 0 0 0 0 0 0 0 0 0 0 0 0 0 0;
        0 0 0 0 0 0 0 0 0 0 0 0 0 0 0 0 0 0 0 0 0;
        0 0 0 0 0 0 0 0 0 0 0 0 0 0 0 0 0 0 0 0 0;
        0 0 0 0 0 0 0 0 0 0 0 0 0 0 0 0 0 0 0 0 0;
        0 0 0 0 0 0 0 0 0 0 0 0 0 0 0 0 0 0 0 0 0;
        0 0 0 0 0 0 0 0 0 0 0 0 0 0 0 0 0 0 0 0 0;
        0 0 0 0 0 0 0 0 -54.64 0 0 0 0 0 0 0 0 0 0 0 0;
        0 0 0 0 0 0 0 0 -54.64 0 0 0 0 0 0 0 0 0 0 0 0;
        0 0 0 0 0 0 0 0 0 0 0 0 0 0 0 0 0 0 0 0 0;
        0 0 0 0 0 0 0 0 0 0 0 0 0 0 0 0 0 0 0 0 0;
        0 0 0 0 0 0 0 0 0 0 -54.64 0 0 0 0 0 0 0 0 0 0;
        0 0 0 0 0 0 0 0 0 0 0 0 0 0 0 0 0 0 0 0 0;
        0 0 0 0 0 0 0 0 0 0 0 0 0 0 0 0 0 0 0 0 0;
        0 0 0 0 0 0 0 0 0 0 -54.64 0 0 0 0 0 0 0 0 0 0;
        0 0 0 0 0 0 0 0 0 0 0 0 0 0 0 0 0 0 0 0 0;
        0 0 0 0 0 0 0 0 0 0 0 0 0 0 0 0 0 0 0 0 0];

colormap('hot')
imagesc(cdata)
colorbar
ylabel('Distance (x 10^2 m)')
xlabel('Distance (x 10^2 m)')
```

#RSS HeatMap (Sensor Position 3)

```
cdata= [0 0 0 0 0 0 0 0 0 0 0 0 0 0 0 0 0 0 0 0 0 0 0;
    0 0 0 0 0 0 0 0 0 0 0 0 0 0 0 0 0 0 0 0 0 0 0;
    0 0 0 0 0 0 0 0 0 0 0 0 0 0 0 0 0 0 0 0 0 0 0;
    0 0 0 0 0 0 0 0 0 0 0 0 0 0 0 0 0 0 0 0 0 0 0;
    0 0 0 0 0 0 0 0 0 0 0 0 0 0 0 0 0 0 0 0 0 0 0;
    0 0 0 0 0 0 0 0 0 0 0 0 0 0 0 0 0 0 0 0 0 0 0;
    0 0 0 0 0 0 0 0 0 0 0 0 0 0 0 0 0 0 0 0 0 0 0;
    0 0 0 0 0 0 0 0 0 0 0 0 0 0 0 0 0 0 0 0 0 0 0;
    0 0 0 0 0 0 0 0 0 0 0 0 0 0 0 0 0 0 0 0 0 0 0;
    0 0 0 0 0 0 0 0 0 0 0 0 0 0 0 0 0 0 0 0 0 0 0;
    0 0 0 0 0 0 0 0 0 0 0 0 0 0 0 0 0 0 0 0 0 0 0;
    0 0 0 0 0 0 0 0 0 0 0 0 0 0 0 0 0 0 0 0 0 0 0;
    0 0 0 0 0 0 0 0 0 0 0 0 0 0 0 0 0 -55.67 0 0 0 0 0;
    0 0 0 0 0 0 0 0 0 0 0 0 0 0 0 0 0 0 0 0 0 0 0;
    0 0 0 0 0 0 0 0 0 0 0 0 0 0 0 0 0 0 0 0 0 0 0;
    0 0 0 0 0 0 0 0 0 0 0 0 0 0 0 0 0 0 0 0 0 0 0;
    0 0 0 0 0 0 0 0 0 0 0 0 0 0 0 0 0 0 0 0 0 0 0;
    0 0 0 0 0 0 0 0 0 0 0 0 0 0 0 0 0 0 0 0 0 0 0;
    0 0 0 0 0 0 0 0 0 0 0 0 0 0 0 0 0 0 0 0 0 0 0;
    0 0 0 0 0 0 0 0 0 0 0 0 0 0 0 0 0 0 0 0 0 0];

colormap('hot')
imagesc(cdata)
colorbar
ylabel('Distance (x 10^2 m)')
xlabel('Distance (x 10^2 m)')
```

#RSS HeatMap (All 3 Sensor Positions)

```
cdata= [0 0 0 0 0 0 0 0 0 0 0 0 0 0 0 0 0 0 0 0 0 0 0 0 0 0;
        0 0 0 0 0 0 0 0 0 0 0 0 0 0 0 0 0 0 0 0 0 0 0 0 0 0;
        0 0 0 0 0 0 0 0 0 0 0 0 0 0 0 0 0 0 0 0 0 0 0 0 0 0;
        0 0 0 0 0 0 0 0 0 0 0 0 0 0 0 0 0 0 0 0 0 0 0 0 0 0;
        0 0 0 0 0 0 0 0 0 0 0 0 0 0 0 0 0 0 0 0 0 0 0 0 0 0;
        0 0 0 0 0 0 0 0 0 0 0 0 0 0 0 0 0 0 0 0 0 0 0 0 0 0;
        0 0 0 0 0 0 0 0 0 0 0 0 0 0 0 0 0 0 0 0 0 0 0 0 0 0;
        0 0 0 0 0 0 0 0 0 0 0 0 0 0 0 0 0 0 0 0 0 0 0 0 0 0;
        0 0 0 0 0 0 0 0 0 0 0 0 0 0 0 0 0 0 0 0 0 0 0 0 0 0;
        0 0 0 0 0 0 0 0 0 0 0 0 0 0 0 0 0 0 0 0 0 0 0 0 0 0;
        0 0 0 0 0 0 0 -54.64 0 0 0 0 0 0 0 0 0 0 0 0 0 0 0 0 0 0 0;
        0 0 0 0 0 -52.64 0 0 0 -54.64 0 0 0 0 0 0 0 0 0 0 0 0 0 0 0;
        0 0 0 0 0 0 0 0 0 0 0 0 0 -55.67 0 0 0 0 0 0 0 0 0 0 0 0 0;
        0 0 0 0 0 0 0 0 0 0 0 0 0 0 0 0 0 0 0 0 0 0 0 0 0 0;
        0 0 0 0 0 0 0 0 -52.64 0 0 -54.64 0 0 0 0 0 0 0 0 0 0 0 0;
        0 0 0 0 0 0 0 0 0 0 0 0 0 0 0 0 0 0 0 0 0 0 0 0 0 0;
        0 0 0 0 0 0 0 0 -52.64 0 0 0 0 0 0 0 0 0 0 0 0 0 0 0;
        0 0 0 0 0 0 0 0 0 0 0 0 0 -54.64 0 0 0 0 0 0 0 0 0 0;
        0 0 0 0 0 0 0 0 0 0 0 0 0 0 0 0 0 0 0 0 0 0 0 0 0 0;
        0 0 0 0 0 0 0 0 0 0 0 0 0 0 0 0 0 0 0 0 0 0 0 0 0 0];

colormap('hot')
imagesc(cdata)
colorbar
ylabel('Distance (x 10^2 m)')
xlabel('Distance (x 10^2 m)')
```

#RSS HeatMap (All 3 localized Sensor Positions)

```
cdata= [0 0 0 0 0 0 0 0 0 0 0 0 0 0 0 0 0 0 0 0 0 0;
        0 0 0 0 0 0 0 0 0 0 0 0 0 0 0 0 0 0 0 0 0 0;
        0 0 0 0 0 0 0 0 0 0 0 0 0 0 0 0 0 0 0 0 0 0;
        0 0 0 0 0 0 0 0 0 0 0 0 0 0 0 0 0 0 0 0 0 0;
        0 0 0 0 0 0 0 0 0 0 0 0 0 0 0 0 0 0 0 0 0 0;
        0 0 0 0 0 0 0 0 0 0 0 0 0 0 0 0 0 0 0 0 0 0;
        0 0 0 0 0 0 0 0 0 0 0 0 0 0 0 0 0 0 0 0 0 0;
        0 0 0 0 0 0 0 0 0 0 0 0 0 0 0 0 0 0 0 0 0 0;
        0 0 0 0 0 0 0 0 0 0 0 0 0 0 0 0 0 0 0 0 0 0;
        0 0 0 0 0 0 0 0 0 0 0 0 0 0 0 0 0 0 0 0 0 0;
        0 0 0 0 0 0 0 0 0 0 0 0 0 0 0 0 0 0 0 0 0 0;
        0 0 0 0 0 0 0 0 0 0 0 0 0 0 0 0 0 0 0 0 0 0;
        0 0 0 0 0 0 0 0 0 0 0 0 0 -55.67 0 0 0 0 0 0 0 0;
        0 0 0 0 0 0 0 0 0 0 0 0 0 0 0 0 0 0 0 0 0 0;
        0 0 0 0 0 0 0 0 0 0 0 -54.64 0 0 0 0 0 0 0 0 0 0;
        0 0 0 0 0 0 0 0 0 0 0 0 0 0 0 0 0 0 0 0 0 0;
        0 0 0 0 0 0 0 0 0 -52.64 0 0 0 0 0 0 0 0 0 0 0 0;
        0 0 0 0 0 0 0 0 0 0 0 0 0 0 0 0 0 0 0 0 0 0;
        0 0 0 0 0 0 0 0 0 0 0 0 0 0 0 0 0 0 0 0 0 0;
        0 0 0 0 0 0 0 0 0 0 0 0 0 0 0 0 0 0 0 0 0 0];
```

```
colormap('hot')
imagesc(cdata)
colorbar
ylabel('Distance (x 102 m)')
xlabel('Distance (x 102 m)')
```

#Calculations involving Arcs and Lines

```
function h = circle(x,y,r)
hold on
th = 0:pi/50:2*pi;
xunit = r * cos(th) + x;
yunit = r * sin(th) + y;
h = plot(xunit,yunit);
hold off
```

```
function h = arc(x,y,r)
hold on
th = 0:pi/50:pi/2;
xunit = r * cos(th) + x;
yunit = r * sin(th) + y;
h = plot(xunit,yunit);
hold off
```

```
figure
arc(0,0,10.121794);
arc(0,0,12.742584);
arc(0,0,sqrt(238.5));
circle(13.2098,8,sqrt(8));
circle(13.7659,7,sqrt(8));
circle(10.4850,7.2414,sqrt(8));
circle(11.6837,5.0857,sqrt(8));
axis equal
title('Calculations');
xlabel('distance(m)');
ylabel('distance(m)');
```

```

figure
arc(0,0,10.121794);
arc(0,0,12.742584);
arc(0,0,sqrt(238.5));

hold on
x=[0,13.2098]; y=[0,8];
plot(x,y)
plot(x,y,'ro')
x=[0,13.7659]; y=[0,7];
plot(x,y)
plot(x,y,'ro')

x=[0,8]; y=[0,9.9183];
plot(x,y)
plot(x,y,'ro')
x=[0,12.5847]; y=[0,2];
plot(x,y)
plot(x,y,'ro')

x=[0,5]; y=[0,8.8006];
plot(x,y)
plot(x,y,'ro')
x=[0,9.6670]; y=[0,3];
plot(x,y)
plot(x,y,'ro')

hold off
axis equal
title('Calculations');
xlabel('distance(m)');
ylabel('distance(m)');

```

```

figure
arc(0,0,10.121794);
arc(0,0,12.742584);
arc(0,0,sqrt(238.5));

hold on
x=[0,13.2098]; y=[0,8];
plot(x,y)
plot(x,y,'ro')
x=[0,13.7659]; y=[0,7];
plot(x,y)
plot(x,y,'ro')

x=[0,10.4850]; y=[0,7.2414];
plot(x,y)
plot(x,y,'ro')
x=[0,11.6837]; y=[0,5.0857];
plot(x,y)
plot(x,y,'ro')

x=[0,7.7538]; y=[0,6.5061];
plot(x,y)
plot(x,y,'ro')
x=[0,9.6180]; y=[0,3.1537];
plot(x,y)
plot(x,y,'ro')

hold off
axis equal
title('Calculations');
xlabel('distance(m)');
ylabel('distance(m)');

```

(C Language)

#RSS Grid Selection

```
#include <stdio.h>
```

```
#include <math.h>
```

```
int row, column, increment = 0;
```

```
double heatMapX[20][20] = {
```

```
{-58.50, -58.86, -65.50, -65.50, -64.77, -64.77, -63.98, -62.59, -64.90, -65.80, -69.00, -71.00, -77.00, -77.30, -75.23, -75.70, -76.10, -76.60, -80.20, -60.44},
```

```
{-58.46, -58.40, -68.50, -68.20, -66.67, -64.02, -63.53, -63.30, -58.93, -58.93, -59.13, -59.28, -70.00, -80.00, -85.00, -90.00, -90.00, -88.00, -88.00, -60.40},
```

```
{-57.02, -57.00, -67.00, -65.00, -64.00, -63.81, -58.71, -58.11, -58.89, -58.80, -58.93, -58.64, -70.00, -80.00, -85.00, -78.00, -85.00, -85.00, -88.00, -60.35},
```

```
{-56.93, -56.81, -62.35, -63.00, -63.50, -63.70, -58.68, -58.30, -58.05, -58.19, -58.50, -58.12, -70.00, -80.00, -85.00, -78.00, -85.00, -87.00, -87.00, -60.33},
```

```
{-56.59, -56.59, -88.00, -90.00, -84.00, -63.10, -58.87, -57.82, -57.82, -57.59, -58.10, -58.41, -58.12, -58.93, -59.14, -59.33, -59.72, -59.81, -59.92, -60.31},
```

```
{-56.17, -56.00, -81.00, -90.00, -90.00, -57.92, -56.60, -57.00, -57.09, -57.75, -57.51, -58.01, -58.23, -58.50, -58.93, -59.03, -59.33, -59.72, -59.75, -60.29},
```

```
{-55.25, -54.60, -54.00, -55.00, -76.00, -59.01, -55.89, -56.55, -56.57, -56.83, -57.09, -57.49, -57.87, -58.20, -58.50, -58.93, -59.13, -59.33, -59.74, -60.15},
```

```
{-55.00, -54.60, -54.00, -53.00, -53.00, -56.00, -55.88, -55.54, -55.92, -56.46, -56.83, -56.44, -57.34, -57.87, -58.17, -58.38, -58.93, -59.13, -59.63, -60.12},
```

```
{-54.07, -53.01, -53.01, -53.01, -53.01, -53.68, -54.76, -55.41, -55.54, -55.94, -56.12, -56.83, -56.54, -57.59, -58.33, -58.70, -58.71, -59.11, -59.33, -60.09},
```


{-53.31, -53.31, -53.31, -53.31, -53.69, -54.07, -54.42, -54.76, -55.08, -55.41, -55.89, -56.12, -56.88, -57.01, -57.59, -58.52, -58.61, -58.72, -59.11, -59.72},

{-52.48, -52.48, -52.48, -52.48, -52.89, -53.31, -53.69, -54.07, -54.76, -55.08, -55.41, -56.00, -56.33, -57.03, -57.64, -57.59, -58.66, -58.73, -59.11, -59.72},

{-51.56, -51.56, -51.56, -51.56, -52.02, -52.48, -53.31, -53.69, -54.07, -54.76, -55.08, -55.34, -56.00, -56.57, -57.09, -57.64, -90.00, -90.00, -90.00, -59.33},

{-50.55, -50.55, -50.55, -50.55, -51.56, -52.02, -52.48, -52.89, -53.69, -54.07, -54.76, -55.41, -55.54, -55.77, -56.57, -90.00, -90.00, -90.00, -59.33},

{-49.38, -49.38, -49.38, -49.97, -50.55, -51.56, -51.56, -52.48, -53.31, -53.69, -54.42, -54.76, -55.41, -56.00, -56.57, -89.00, -90.00, -90.00, -59.33},

{-48.04, -48.04, -48.04, -49.38, -49.38, -50.55, -51.56, -51.56, -52.48, -53.31, -54.07, -54.76, -55.08, -55.54, -57.70, -89.00, -90.00, -90.00, -59.00},

{-46.46, -46.46, -46.46, -48.04, -48.71, -49.38, -50.55, -51.56, -52.02, -52.89, -53.69, -54.42, -54.76, -55.41, -56.67, -59.00, -90.00, -90.00, -59.00},

{-44.42, -44.52, -44.52, -46.46, -48.04, -49.38, -49.97, -50.55, -51.56, -52.48, -53.31, -54.07, -54.76, -55.41, -56.00, -57.00, -58.00, -58.12, -58.66, -58.76},

{-42.03, -42.03, -44.52, -44.52, -46.46, -48.04, -49.38, -50.55, -51.56, -52.48, -53.31, -54.07, -54.76, -55.41, -56.00, -56.57, -57.23, -57.59, -58.46, -58.76},

{-38.50, -38.50, -42.03, -44.52, -46.46, -48.04, -49.38, -50.55, -51.56, -52.48, -53.31, -54.07, -54.76, -55.41, -56.00, -55.70, -57.19, -57.59, -58.46, -58.76},

{-32.48, -38.50, -42.03, -44.52, -46.46, -48.04, -49.38, -50.55, -51.56, -52.48, -53.31, -54.07, -55.00, -55.55, -56.17, -56.80, -57.19, -57.66, -58.46, -58.76}

};

```

double heatMapY[20][20],heatMap[20][20],temp3,temp4;

void initiate(){
for (row=0;row<20;row++){
for (column=0;column<20;column++){
heatMap[row][column] = 0.00;}}}
void calculate(){
double TSS,RSS,FreeSpacePathLoss,frequency,distance;
printf("\n Enter RSS:\t");
scanf("%lf",&RSS);
increment = increment + 1;

for (row=0;row<20;row++){
for (column=0;column<20;column++){
if (heatMapX[row][column] == RSS){
heatMapY[row][column] = increment;
}
else heatMapY[row][column] = 0.0;
}}}

for (row=0;row<20;row++){
for (column=0;column<20;column++){
heatMap[row][column] = heatMap[row][column] + heatMapY[row][column];
}}}

void display(){
for (row=0;row<20;row++){
printf("\n");
for (column=0;column<20;column++){
printf(" %2.0f",heatMap[row][column]);
}}
printf("\n");
}

```

```

int main(){
int choice; initiate();
do{
printf("\n 1 : Add Sensor Node Information"); printf("\n 2 : Show the Projected Matrix");
printf("\n 3 : Exit"); printf("\n\n What is your Choice?\t");
scanf("%d",&choice);
switch(choice){
case 1 : calculate(); break;
case 2 : display(); break;
case 3 : break;
default : printf("\n Wrong Choice of Input!\n");
}}while(choice!=3);
return 0;
}

```

#Distance Calculation using RSS

```

#include <stdio.h>
#include <math.h>
int main()
{
double TSS,RSS,FreeSpacePathLoss,frequency,distance,temp3,temp4;
TSS = 39.0; frequency = 0.9;
printf("\n Enter RSS:\t");
scanf("%lf",&RSS);
temp3 = TSS - RSS - 20*log10(frequency) - 92.45;
temp4 = temp3 / 20.0;
distance = pow(10.0,temp4);
printf("\n Distance:\t%f Km\n",distance);
printf("\n \t\t%f m\n",distance*1000);
printf("\n \t\t%f unit\n",distance*10);
return 0;
}

```